Binding, sensing, and transporting anions with pnictogen bonds: The case of organoantimony Lewis acids

Brendan L. Murphy and François P. Gabbaï*

Department of Chemistry, Texas A&M University, College Station, Texas 77843-3255, USA.

ABSTRACT: Motivated by the discovery of main group Lewis acids that could compete or possibly outperform the ubiquitous organoboranes, several groups, including ours, have engaged in the chemistry of Lewis acidic organoantimony compounds as new platforms for anion capture, sensing and transport. Principal to this approach are the intrinsically elevated Lewis acidic properties of antimony, which greatly favor the addition of halide anions to this group 15 element. The introduction of organic substituents to the antimony center and its oxidation from the +III to the +V state provides for tunable Lewis acidity and a breadth of applications in supramolecular chemistry and catalysis. The performances of these antimony-based Lewis acids in the domain of anion sensing in aqueous media illustrate the favorable attributes of antimony as a central element. At the same time, recent advances in anion binding catalysis and anion transport across phospholipid membranes speak to the numerous opportunities that lie ahead in the chemistry of these unique main group compounds.

Introduction

Lewis acidic main group compounds have become ubiquitous in both organic and organometallic chemistry as illustrated by the rise perfluorinated triarylboranes[1] and their prevalence in numerous applications.[2] Even if much less reactive than their boron halide counterparts, these organoboranes are limited mostly to use in organic media and often readily decompose in aqueous environments. These water compatibility issues can be resolved, at least in part, by using aryl groups like mesityls to sterically protect the boron center against water.[3] Using this strategy, several groups, including ours, have prepared water-compatible boranes[4] whose solubilities can be enhanced by the introduction of peripheral cationic moieties.[5] These cationic groups can also increase the anion affinity of these boranes, a feature that we have exploited for the sensing of toxic anions such as fluoride and cyanide in aqueous solutions.[6] While these boranes can be used to detect parts-per-million concentrations of these anions, the binding event is typically accompanied by a fluorescence "turn-off" response[7] thereby restricting their analytical practicality as molecular sensors. These boranes also tend to decompose upon standing in aqueous media over time, and their vulnerability to oxidation[8] challenges their longevity under aerobic conditions, especially in the presence of reactive oxygen species.

However, as documented in the early work of Gutmann, Lewis acidity also emerges as a prevalent property of Sb(V) halides. Using the activation of the C-Cl bond of tritylchloride in MeCN as an indicator, Gutmann demonstrated that $SbCl_5$ stands near the apex of his chloride ion affinity scale, second only to $InCl_3$ (**Scheme 1**).[9] In another series of seminal contributions, Olah[10], and later Gillespie,[11] showed that SbF_5 could be used for the activation of C-F bonds in organic compounds or for the generation of "superacids" (**Scheme 1**).[12] As seen in boron chemistry, early reports also suggested that organoantimony derivatives retain some of the Lewis acidic characteristics of their halide analogs while displaying much greater air and water tolerance.[13] Encouraged by these precedents, we posited that such compounds may be uniquely suited for anion binding in a variety of competitive media.

Scheme 1. Classic investigations into the Lewis acidity of antimony compounds.

Gutmann (1962):

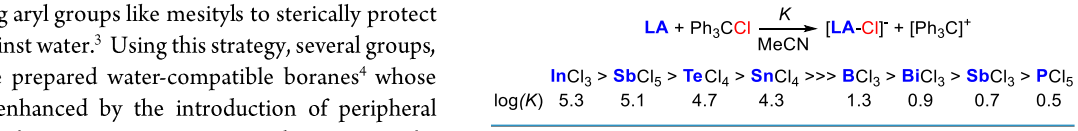

Olah (1964):

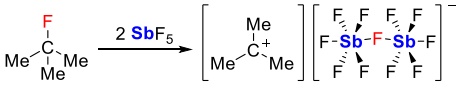

Building off these seminal studies, we have undertaken extensive investigation into the properties and applications of organoantimony compounds in our laboratory. In this Perspective, we will review these efforts while spotlighting other notable works also focused on the development of Lewis acidic organoantimony compounds as new anion binding and trafficking platforms. In doing so, we first discuss the structural and electronic factors that grant antimony its Lewis acidity. We will show how these basic principles have guided design of organoantimony-based anion binding units, with particular attention paid to the development of "turn-on" sensing systems. We will also highlight arising utilities of organoantimony compounds for anion-binding catalysis and as transporters of anions across biological membranes. Finally, because this Perspective will only discuss organic derivatives of antimony, we direct the reader's attention to our adjacent work employing antimony as a coordination non-innocent ligand for late

transition metal centers, in which the antimony center is also capable of anion binding[14] and sensing.[15]

Origin of Lewis acidity in simple antimony compounds and related concepts

The case of antimony (III) derivatives

To understand the origin of the elevated Lewis acidity of antimony compounds compared to lighter group 15 elements, or pnictogens (Pn), we look back to the experimental work of Gutmann, which interrogated the conversion of pnictogen trichlorides ($PnCl_3$) into the corresponding tetrachloropnictate complexes. These pioneering studies showed that the chloride affinity of $SbCl_3$ exceeds that of $AsCl_3$ and far exceeds that of PCl_3 in MeCN.[16] These experimental results are corroborated by computational work by Bickelhaupt and co-workers who applied the activation strain model to clarify the origin of this simple trend.[17] This computational approach, as summarized in **Figure 1**,[18] considers the formation of a complex based on: i)the deformation of the interacting partners to geometries that match those in the final complexes; ii) the formation of the final complex by association of the deformed partners. These two steps give rise to two energy terms, referred to as the strain energy (ΔE_{strain}) and the interaction energy (ΔE_{int}). Furthermore, energy decomposition analysis (EDA) schemes can be used to shed light on how electrostatic forces (ΔV_{elstat}), orbital-based interactions (ΔE_{oi}) and Pauli repulsions (ΔE_{Pauli}) influence ΔE_{int} (**Table 1**).

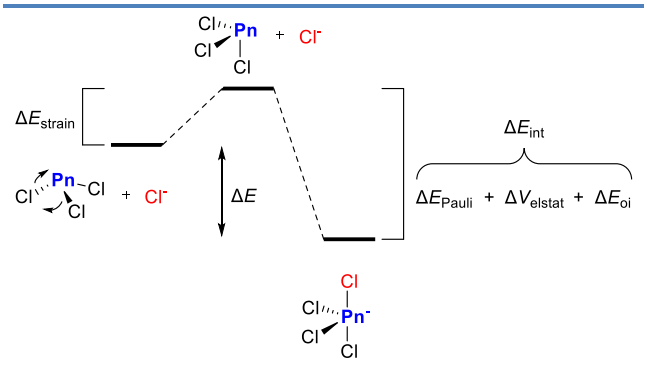

Figure 1. Illustration of the structural and energetic components of chloride binding by Pn(III) centers investigated by Bickelhaupt and co-workers.

Table 1. Energy decomposition analysis of representative Cl^-→$PnCl_3$ interactions.[17] Values are given in kcal·mol^{-1}.

PnB Interaction	ΔE_{strain}	ΔE_{Pauli}	ΔV_{elstat}	ΔE_{oi}	ΔE_{int}	ΔE
Cl^-→PCl_3	14.4	119.2	-84.8	-74.2	−39.8	-25.5
Cl^-→$AsCl_3$	11.3	101.9	-85.5	-62.8	-46.4	-35.1
Cl^-→$SbCl_3$	8.9	100.9	-93.3	-59.2	-51.7	-42.7

First, the ΔE_{strain} needed to distort the Pn(III) center from its ground state geometry to that adopted in the tetrachloropnictate anion is lowest for the antimony derivative. This lower value can be explained by the Cl-Sb-Cl angles in $SbCl_3$ which are close to 90°, as in the corresponding antimonate complex. A slight decrease is also seen in ΔE_{Pauli}, reflecting the larger size of antimony and its ability to more easily accommodate an extra ligand. A more important factor is the electrostatic term (ΔV_{elstat}). The magnitude of this term notably increases down the group, as the electropositivity and polarizability of the Pn center also increases. It follows that $[SbCl_4]^-$ is the most electrostatically stabilized complex of the series. The ΔE_{oi} term is not to be ignored though. Because of the increasing diffuseness and radial nodes of its valence orbitals, the covalency of the newly formed Pn-Cl bond decreases going down the group. Inspection of the values in **Table 1** shows that this decrease is moderate, with the ΔE_{oi} of the antimony system being only marginally more positive than that for arsenic. Altogether, out of the series considered, $SbCl_3$ binds chloride most exothermically. When compared to the arsenic system, the superior Lewis acidity of $SbCl_3$ can be seen as resulting mostly from the more negative ΔV_{elstat} term, with all other terms offsetting one another (**Table 1**).

The case of antimony (V) derivatives

The early work of Gutmann summarized in **Scheme 1** showed that antimony(V) derivatives are more Lewis acidic than their trivalent counterparts.[19] The same study found that $SbCl_5$ is more chloridophilic than PCl_5 by nearly five orders of magnitude,[16] again suggesting that Lewis acidity increases as the group is descended. This conclusion is supported by several computational studies which show that the computed gas-phase fluoride ion affinities (FIAs) of the pnictogen pentafluorides increase from PF_5 to SbF_5 (**Table 2**).[20]

Table 2. Computed gas-phase FIAs of pnictogen pentafluorides, which highlights the elevated fluoridophilicity of SbF_5 compared to its lighter congeners. Values are given in kJ·mol^{-1}.

Pnictogen pentafluoride	FIA[20b]	FIA[20a]	FIA[20c]
PF_5	394	384	385
AsF_5	426	439	436
SbF_5	489	496	492

A recent activation-strain and EDA study investigated fluoride anion binding by Pn(V) derivatives.[21] The data in **Table 3**, compiled for the PnF_5 species, shows that the ΔE_{oi} and ΔV_{elstat} terms become less negative as the group is descended because of the lengthening of the Pn-F linkage and the increased diffuseness of the Pn orbitals. The decrease of these stabilizing interactions is compensated for by the Pauli repulsions which become lower as the size of Pn increases. Owing to the balancing of these opposite influences, ΔE_{int} shows little variation down the group. Thus, through the lens of the activation-strain model, the high Lewis acidity of antimony originates from the lower ΔE_{strain} term which reflects the greater flexibility of SbF_5. With longer and more diffuse Pn-F σ bonds, the fluoride ligands acquire greater freedom of motion and stand further from one another, allowing SbF_5 to more easily accommodate the C_{4v} geometry it displays in $[SbF_6]^-$.

Table 3. Energy decomposition analysis of representative F^-→PnF_5 interactions.[21] Values are given in kcal·mol^{-1}.

PnB Interaction	ΔE_{strain}	ΔE_{Pauli}	ΔV_{elstat}	ΔE_{oi}	ΔE_{int}	ΔE
F^-→PF_5	51.9	230.9	-220.1	-154.1	-143.4	-91.6
F^-→AsF_5	33.0	207.5	-215.1	-129.8	-137.5	-104.5
F^-→SbF_5	23.7	166.7	-209.3	-101.4	-144.1	-120.3

Is a group 15 Lewis acid the same thing as a pnictogen bond donor?

We note that donor-acceptor interactions involving Pn derivatives as acceptors have been known for several decades and

only recently referred to as "pnictogen bonds" (PnBs).[22] Akin to the halogen bond[23] and the chalcogen bond,[24] PnBs are often described as resulting from the interaction of a donor (D) toward a Pn-centered electrophilic "σ hole", a region of positive electrostatic potential opposite to one of the primary bonds (**Figure 2**).[22, 25] In this light, the PnB is often regarded as a "non-covalent" interaction. While such a description may be fitting of cases where the interaction is weak, it presents the danger of oversimplifying the nature of PnBs. Namely, this characterization ignores the contribution of orbital-based interactions, like those identified in the above-mentioned work of Bickelhaupt.[18] Such orbital-based interactions were discussed in no uncertain terms in the early work of Alcock[26] who in 1972 identified the ability of main group element-centered σ* orbitals to accept electron density from filled donor orbitals (**Figure 2**). This concept was revisited by Norman in the specific case of pnictogen derivatives in 1994.[27] This notion is also prevalent in the seminal work of Scheiner from 2011 on the weakly associated $H_3N{\rightarrow}PH_3$ adduct in which the nitrogen lone pair aligns with one of the primary P-H bonds and transfer some of its density into the corresponding P–H σ* lobe.[28] The importance of such orbital or charge transfer interactions will depend on the nature of both the donor and the Pn acceptor. It can be weak as in the $H_3N{\rightarrow}PH_3$ adduct or strong as in $X^-{\rightarrow}PnX_3$ adducts in which the newly formed $X^-{\rightarrow}Pn$ bond displays considerable covalency. It follows that the "non-covalent" adjective as a descriptor of PnBs loses its legitimacy.[18] PnBs are simply examples of dative bonds,[29] connecting a donor to a group 15 acceptor ([Pn]), stabilized through the interplay of Coulombic and covalent or orbital-based interactions with possible contribution from dispersion interactions. We therefore consider that any D→[Pn] complex can also be described as a Lewis adducts and a PnB donor as a Lewis acid.

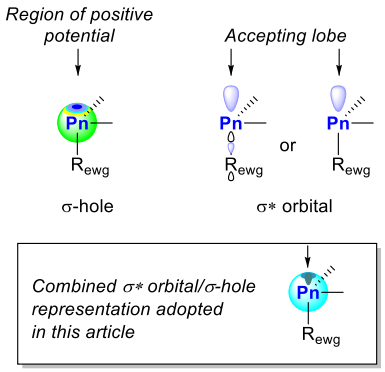

Figure 2. Schematic representations of the "σ hole" (left) and the σ* orbital of a trivalent pnictogen. The σ* orbital is presented in a simplified fashion, with the second representation only keeping the accepting lobe. A similar picture could be drawn for a pentavalent pnictogen. R_{ewg} = electron-withdrawing substituent.

Anion complexation chemistry

Antimony (III) compounds

The Lewis acidity of antimony persists despite the passivating effect of an aryl appendage. Indeed, simple arylantimony(III) dihalide species are sufficiently Lewis acidic to form isolable antimonate complexes. Such is the case of $PhSbCl_2$ (**1**), which exists in the solid-state as a weak contact aggregate[30] and reacts with chloride to form the bridged dianion ($[\mathbf{1}\text{-}(\mu\text{-}Cl)_2\text{-}\mathbf{1}]^{2-}$, **Scheme 2**).[31] Each antimony(III) center of this centrosymmetric dimer adopts a local square pyramidal geometry with pairs of chloride ligands in *trans* positions to each other. The disposition of these two chloride ligands can be viewed as resulting from their addition to the sites featuring the deepest σ holes and the most energetically accessible σ* orbitals. Moreover, treating **1** with two equivalents of chloride gives rise to the monomeric, square pyramidal-shaped dianion ($[\mathbf{1}\text{-}2Cl]^{2-}$, further indicating that both binding sites are accessible to an incoming chloride.[31a]

Similarly, diarylantimony(III) halide species have also been shown to display notable Lewis acidity, and are also capable of Lewis base recognition at a binding site that is also *trans* to the halide ligand.[32] For example, the monomeric Ph_2SbCl (**2**)[33] also reacts with chloride anions to form $[Ph_2SbCl_2]^-$ ($[\mathbf{2}\text{-}Cl]^-$, **Scheme 2**), which takes on a seesaw geometry with the two chloride ligands *trans* to each other.[31a, 34] To our knowledge, the dianionic $[\mathbf{2}\text{-}2Cl]^{2-}$ has never been isolated, pointing to the inaccessibility of the σ hole/σ*-orbital *trans* from a phenyl group.

Scheme 2. Chloride complexation by chlorostibines 1 and 2.

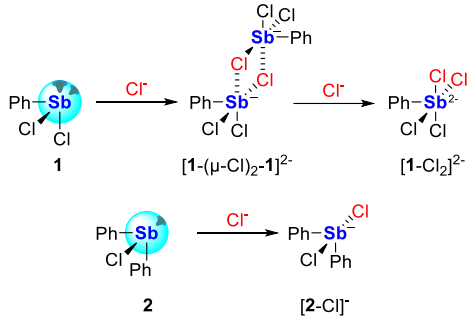

Complete arylation of the antimony(III) center typically limits the chemistry of triarylstibines to use as an L type ligand in coordination chemistry.[35] However, the introduction of electron-withdrawing aryl groups can elicit PnB donor properties at the antimony center. Such is the case of $(C_6F_5)_3Sb$ (**3**), which forms a structurally characterized adduct with Ph_3PO.[19] The Lewis acidic behavior of **3** also manifests in its affinity for chloride anions, as reported by Matile.[36] ^{19}F NMR titration with tetrabutylammonium chloride (TBACl) in d_8-THF affords a chloride association constant ($K(Cl^-)$) of 53,000 M^{-1}. Lower chloride binding is observed in the case of $Ph(C_6F_5)_2Sb$ (**4**, $K(Cl^-)$ = 1,800 M^{-1}), while $Ph_2(C_6F_5)Sb$ (**5**) shows no measurable affinity for the ionic guest, pointing the crucial role played by number of pentafluorophenyl substituents appended to the antimony center (**Figure 3**).

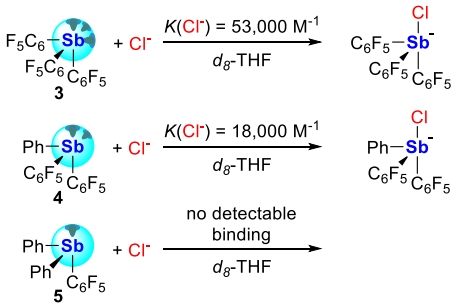

Cl^- binding constant ($K(Cl^-)$) for homoleptic Ar_3Sb derivatives

Cpd	Ar	$K(Cl^-)$	Cpd	Ar	$K(Cl^-)$
6	3,5-$F_2C_6H_3$	61 ± 2 M^{-1}	**10**	4-$NO_2C_6H_4$	94 ± 2 M^{-1}
7	3,5-$Cl_2C_6H_3$	52 ± 1 M^{-1}	**11**	4-CNC_6H_4	36 ± 2 M^{-1}
8	3,4,5-$F_3C_6H_2$	253 ± 3 M^{-1}	**12**	3,5-$(CF_3)_2C_6H_3$	702 ± 16 M^{-1}
9	3,4,5-$Cl_3C_6H_2$	341 ± 6 M^{-1}	**13**	Ph	no binding

Figure 3. Top: Chloride binding constants of stibines **3**-**5** as determined by Matile. Bottom: Chloride binding constants of homoleptic stibines **6**-**13** as determined by Beer.

Recent work by the group of Beer further illustrates the benefits resulting from introducing electron-withdrawing units on Ar_3Sb systems (**Figure 3**).[37] Indeed, **6-12** all bind chloride in d_8-THF as indicated by ^1H NMR spectroscopy. Chloride binding peaks in the case of **12**, which bears the most electron deficient aryl rings of the compounds studied and possesses a $K(Cl^-)$ of 702 ± 16 M^{-1}. Moreover, the chloride affinity of **12** was markedly higher than its affinity for Br^-, I^-, and NO_3^-, and more basic anions like OAc^-, OCN^-, and NO_2^- were found to bind more weakly than Cl^-. We will note in passing a possible disconnect in the magnitude of the chloride binding constants measured by the Matile and Beer groups since the C_6F_5 and the 3,5-$(CF_3)_2C_6H_3$ aryl groups have similar electron-withdrawing properties when appended to main group Lewis acids. It is also worth noting that Ph_3Sb (**13**) showed no measurable affinity for chloride in d_8-THF.

Anion binding has also been investigated by the Cozzolino group using oxygen-bridged bidentate distibines[38] such as **14** which displays halide binding constants in CH_2Cl_2 of $8.7 \times 10^5 \pm 0.98 \times 10^5$ M^{-1}, $1.69 \times 10^4 \pm 0.5 \times 10^4$ M^{-1}, $2.39 \times 10^3 \pm 1.47 \times 10^3$ M^{-1} for chloride, bromide, and iodide, respectively (**Figure 4**).[39] In addition to showing halide anion binding selectivity, **14** also interacts with the cyanide and effectively promotes its phase transfer for application in cyanation chemistry.

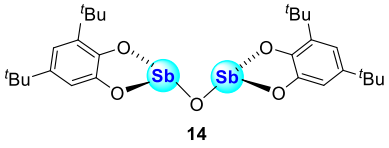

14

Figure 4. Structure of bidentate distibine **14**.

Antimony (V) compounds – Halostiboranes

Harkening back to initial studies on the anion binding chemistry of antimony (**Scheme 1**), Gutmann found that $SbCl_5$ possesses a chloridophilicity that is nearly five orders of magnitude greater than that of $SbCl_3$.[9] The increased Lewis acidity observed upon oxidation can be correlated to a deepening of the σ hole at the antimony as well as a lowering in the energy of the σ* orbital aligned with an incoming Lewis base, as illustrated in **Figure 5**.[19] These effects, which have been examined in the special case of **3** and its corresponding tetrachlorocatecholatostiborane (*vide infra*),[19] should apply to any pair of antimony Lewis acids differentiated by the +III or +V oxidation state of the antimony center.

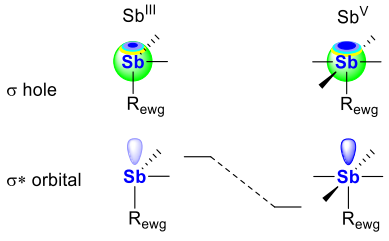

Figure 5. Deepening of the σ hole and stabilization of the σ* orbital resulting from oxidation of an Sb(III) species to an Sb(V) species.

The Lewis acidity of the Sb(V) compounds can be observed in arylated derivatives such as $PhSbCl_4$ (**15**) and Ph_2SbCl_3 (**16**), which readily form the corresponding chloroantimonate species $[PhSbCl_5]^-$ ([**15**-Cl]$^-$)[40] and $[Ph_2SbCl_4]^-$ ([**16**-Cl]$^-$)[41] when treated with an appropriate chloride salt (**Scheme 3**). The formation of these salts may be seen as mirroring that of their +III analogues, namely the $[PhSbCl_3]^-$ anion ([**1**-Cl]$^-$) and $[Ph_2SbCl_2]^-$ anion ([**2**-Cl]$^-$) (**Scheme 2**). Even if direct comparisons of these Lewis acids are not available in the literature, the antimony(V) derivatives **15** and **16** should display greater Lewis acidic properties than their trivalent counterparts.

Scheme 3. Chloride complexation by halostiboranes 15 and 16.

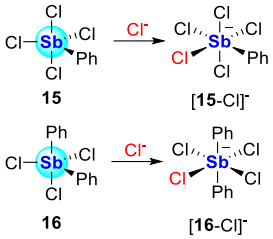

Further substitution of the antimony center by aryl substituents can be anticipated to negatively affect its Lewis acidity. These deleterious effects are already evident when analyzing the behavior of Ph_3SbCl_2, which to our knowledge does not associate with chloride ions. On the other hand, Ph_3SbF_2 (**17**), which contains smaller and more electron-withdrawing ligands, complexes fluoride in $CDCl_3$ to form $[Ph_3SbF_3]^-$ ([**17**-F]$^-$, **Scheme 4**) as verified by ^{19}F NMR.[42] A stronger complexation was observed in the case of $(C_6F_5)_3SbF_2$ (**18**), leading to the unambiguous characterization of $[(C_6F_5)_3SbF_3]^-$ ([**18**-F]$^-$) formed by addition of CsF to **18** in MeOH.[43] Another strategy to elevate the anion affinity of triaryldihalostiboranes rests on the introduction of hydrogen bonding (HB) groups, as in the case **19**, a complex featuring two *N*-(2,6-difluorophenyl-*o*-aminophenyl)phenyl groups. Our investigation of this derivative shows that it outcompetes Ph_3SbF_2 for fluoride binding in $CDCl_3$ at -30 °C.[42]

Scheme 4. Fluoride complexation by triaryldihalostiboranes 17-19.

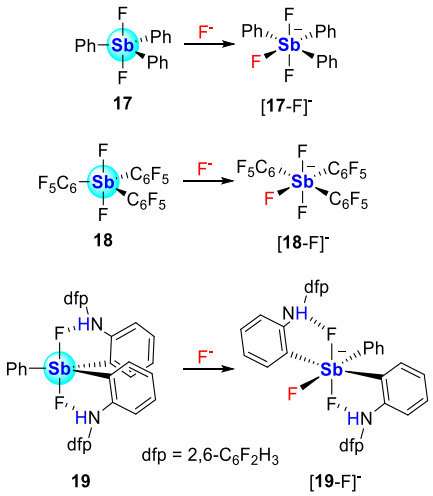

Anion complexation could also be achieved by pentacoordinate antimony(V) systems in which the antimony center is bound to two doubly deprotonated 2,2,2,2',2',2'-hexafluorocumylalcohol C,O-

bidendate ligands.[44] Indeed, the antimony(V) derivative **20** was shown to complex fluoride anions, as verified by the structural characterization of [**20**-F][Et_4N]. Interestingly, variable temperature ^{19}F NMR studies reveal that [**20**-F]$^-$ exists as several structural isomers at -40 °C, suggesting that the fluoride anion can reversibly sample the various anion binding sites presented by **20** (**Scheme 5**). Addition of water to an acetone solution of [**20**-F]$^-$ induces decomplexation of the fluoride anion, reminding us of its high hydration energy (-504 kJ·mol^{-1}).

Scheme 5. Reversible fluoride binding behavior of stiborane 20 upon introduction of water.

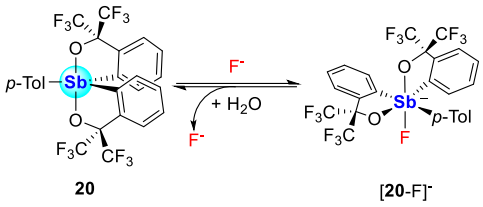

Antimony (V) compounds - Catecholatostiboranes

Monofunctional systems

The imposition of geometrical constraints is also an effective way to enhance the Lewis acidity of antimony derivatives. One of the earliest pieces of evidence for these effects was provided in the case of $Ph_3SbO_2C_6H_4$ (**21**, **Scheme 6**) that, based on X-ray analysis, engages a water molecule *via* formation of an O→Sb bond of 2.51 Å.[13b] The formation of such a water adduct is not observed for Ph_3SbF_2 and Ph_3SbCl_2, pointing to the role of the structural constraints imposed by the SbO_2C_2 five-membered ring in elevating the Lewis acidity of the antimony(V) center *via* distortion of its ground state geometry. Another favorable feature of catecholate groups is their minimal steric profile since the coordinating oxygen ligands extend out from the aromatic backbone and thus partly escape its steric hindrance. The formation of [**22**-Cl][Et_3NH] by reaction of Ph_3SbCl_2 with 2,3-naphthalenediol and Et_3N is another important precedent directly relevant to the topic of this Perspective since it involves the complexation of a halide anion (**Scheme 6**).[45] The formation of [**22**-Cl]$^-$ contrasts with the lack of Lewis acidity in Ph_3SbCl_2.

Scheme 6. Top: water complexation by catecholatostiborane 21. Bottom: synthesis of [22-Cl][Et$_3$NH] from Ph$_3$SbCl$_2$.

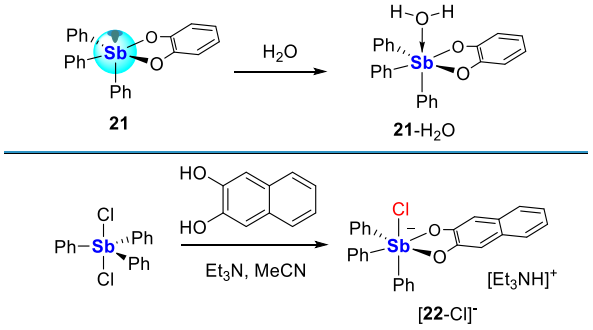

In addition to their elevated Lewis acidity, catecholatostiboranes also benefit from their ease of preparation. In addition to metathesis reactions such as that used to form **22**, these species can also be obtained through the simple combination of a triarylstibine with an *ortho*-quinone such as *o*-chloranil. Owing to its perchlorination, this quinone is a particularly potent oxidant that engages a range of organoantimony compounds, including **13** which is readily converted into $Ph_3SbO_2C_6Cl_4$ (**23**, **Figure 6**) as demonstrated by Holmes in 1987.[45] Our reinvestigation of this compound shows that, unlike its trivalent precursor, it behaves as a potent Lewis, able to bind a fluoride anion when treated with [TBA][Ph_3SiF_2] (TBAT). The formation of [**23**-F][TBA] took place in CH_2Cl_2 and survived aqueous workup, speaking to the stability of the Sb-F bond.[46] The solid-state structure of [**23**-F]$^-$ displays a short Sb-F bond distance of 1.9877(13) Å (**Figure 6**), only slightly longer than the average Sb-F bond length in [SbF_6]$^-$ (1.844 Å).[47] As noted at the start of this section, we have explained the increased Lewis acidity observed upon oxidation by a lowering of σ* orbital by almost 1.1 eV and a deepening of the σ hole.[19] These effects, combined with the structural predisposition resulting from the presence of a SbO_2C_2 five-membered ring may serve to rationalize the anion affinity of molecules such as **23**.

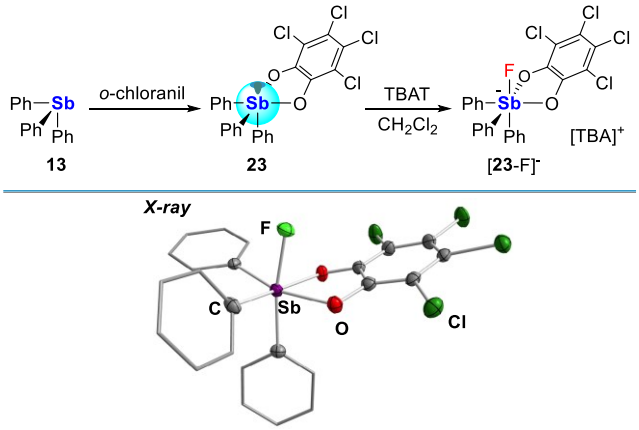

Figure 6. Top: Oxidation of stibine **13** following treatment with *o*-chloranil to yield catecholatostiborane **23**, and isolation of [**23**-F][TBA] upon treatment of **23** with TBAT. Bottom: Solid-state structure of [**23**-F]$^-$.

Altogether, the conversion of **13** into **23** establishes a simple approach for converting Lewis basic triarylstibines into Lewis acidic stiboranes. We found that even electron poor stibines such as $(C_6F_5)_3Sb$ (**3**) and $(3,5\text{-}(CF_3)_2C_6H_3)_3Sb$ (**12**) could be converted into the corresponding tetrachlorocatecholatostiboranes **24** and **25** (**Figure 7**).[19] As is the case for the parent triphenyl derivative, the antimony-centered LUMO is stabilized by 0.89 eV and 0.78 eV upon formation of **24** and **25**, respectively. A sizable increase in the FIA values (δ(FIA)) was also computed for these three pairs of compounds upon oxidation of the antimony center. The largest change was observed in the case of the parent derivative **13** whose FIA increases by δ(FIA) = 150 kJ·mol^{-1} upon conversion into **23** versus 111 kJ·mol^{-1} and 132 kJ·mol^{-1} for the **3**/**24** and **12**/**25** couples, respectively. This strategy has been applied by Matile on other fluorinated triarylstiboranes including $(3,4,5\text{-}F_3C_6H_2)_3Sb$ (**8**), which was readily converted into the corresponding tetrachlorocatecholatostiborane **26**.[48] We should also point out the growing role that perhalogenated catecholate groups are playing in the chemistry of arsenic,[49] silicon,[50] germanium[51] and phosphorus Lewis acids.[49, 52]

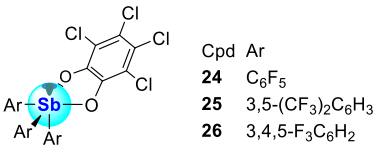

Figure 7. Structures of catecholatostiboranes **24**-**26**.

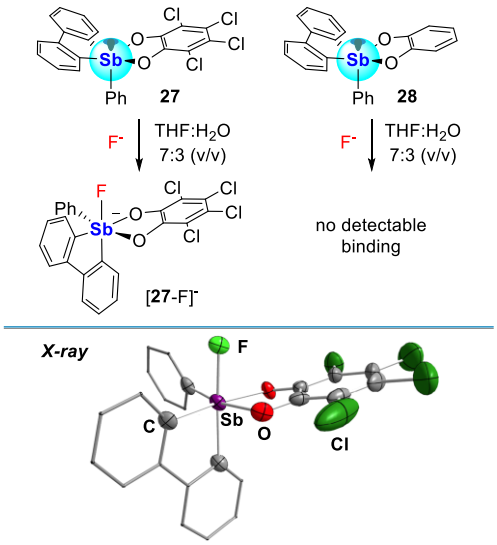

Figure 8. Top: Fluoride binding behaviors of catecholatostiboranes **27** and **28** in THF:water (7:3 (v/v)). Bottom: Solid-state structure of [**27**-F]$^-$.

We have also aimed to assess the influence of catecholate perchlorination on the Lewis acidity of the antimony center. For example, we decided to compare the anion affinity of **27**, first reported by Holmes,[45] to that of the perprotiocatecholate analogue **28**. We found that **27** displays a high binding constant for the fluoride anion ($K(F^-)$ of 13,500 ± 1,400 M^{-1} in THF:water (7:3 (v/v)) as established by a UV-vis titration while **28** shows no affinity for the anion under the same conditions (**Figure 8**).[53] The contrasting behaviors of these two compounds underscore how important the electronic features of the catecholate are in governing the anion affinity of these compounds. In this case, perchlorination of the catecholate most likely reduces the donicity of the oxygen atoms, leaving a more exposed and thus more Lewis acidic antimony(V) center. The anionic complex [**27**-F]$^-$, which has been characterized as a tris(dimethylamino)sulfonium ([TAS]$^+$) salt, displays a short Sb-F bond length of 1.973(4) Å, on par with that of the aforementioned [**23**-F]$^-$.[53] In addition to demonstrating the importance of catecholate perchlorination, **27** may also benefit from its bicyclic structure. The integration of two antimony-fused five membered rings most likely accentuates the geometrical constraints imposed on the ground state structure, elevating its Lewis acidity.[54]

Bifunctional systems

The facility by which tetrachlorocatecholatostiboranes can be prepared prompted us to investigate their introduction in more elaborated scaffolds, including bifunctional ones that would support anion chelation.[4b, 4c, 6, 55] To explore this possibility, we synthesized the 4,5-bis(diphenylantimony)-9,9-dimethylxanthene (**29**) and found that it could be easily converted into **30** (**Figure 9**).[46] A structural analysis of **30** shows that the two square-pyramidal stiborane units orient their basal square face inward, thus defining a binding pocket possibly adapted to the capture of small anions. Another favorable feature of this derivative lies in the nature of its LUMO, which spans the two antimony atoms and displays significant σ*(Sb-C/O) parentage with lobes extending towards the center of the binding pocket.

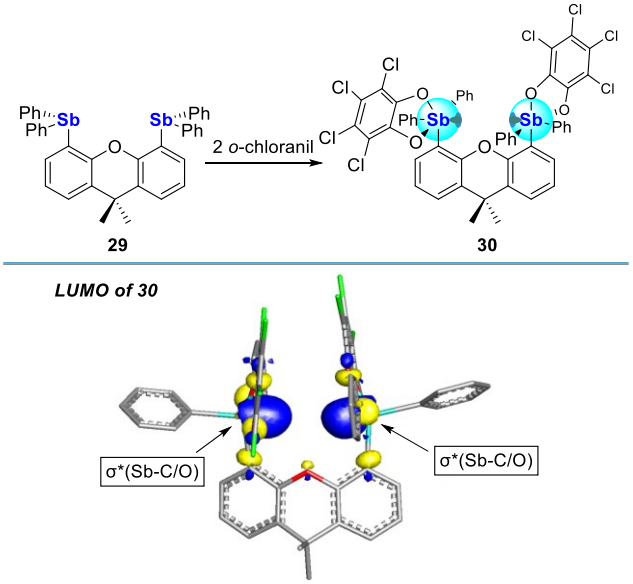

Figure 9. Top: Oxidation of distibine **29** to distiborane **30** following treatment with two equivalents of *o*-chloranil. Bottom: Contour plot of the LUMO (isovalue: 0.05) of **30** showing the projection of the σ*(Sb-C/O) orbitals into the binding pocket.

Congruent with these attributes, **30** readily complexes a fluoride anion to afford [**30**-F]$^-$ (**Figure 10**). A crystal structure of its

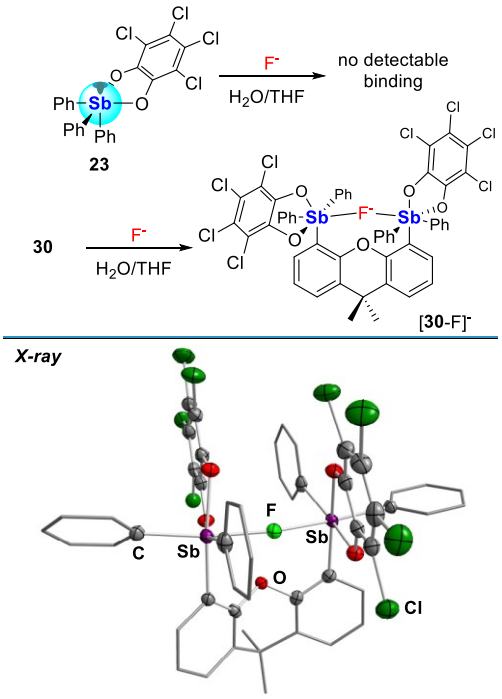

Figure 10. Top: Fluoride binding behaviors of **23** and **30** in water-THF (9.5:0.5 (v/v), 10 mM citrate, 45 mM Triton X-100). Bottom: Solid-state structure of [**30**-F]$^-$.

[TBA]$^+$salt confirms the formation of a fluoride chelate complex supported by two Sb-F bonds of 2.1684(19) Å and 2.1621(19) Å.[46] This distance shows a measurable elongation when compared to the value of 1.9877(13) Å found for the terminal Sb-F bond in [**23**-F]$^-$, in line with the μ_2 coordination mode of the fluoride anion in [**30**-F]$^-$. The thermodynamic impact of anion chelation manifests in the acidity constant (pK_{Sb}) of the antimony center, which is equivalent to the pH at which 50% of the antimony Lewis acid is neutralized by a hydroxide anion. Indeed, the pK_{Sb} of **30** (5.8 ± 0.1) measured in water:THF (9.5:0.5 (v/v), 10 mM sodium phosphate, 45 mM Triton X-100) is significantly lower than that of **23** (7.4 ± 0.1). In line with this result, whereas **30** is capable of binding fluoride in a highly competitive water:THF (9.5:0.5 (v/v), pH 4.34, 10 mM citrate, 45 mM Triton X-100) solution with a $K(F^-)$ value of 700 ± 30 M^{-1}, **23** does not engage the fluoride anion in that medium.

Despite its promising attributes, fluoride chelation by **30** positions the bound fluoride above the oxygen of the xanthene backbone, leading to a repulsive O···F$^-$ interaction that likely dampens the anion affinity of the chelator. To circumvent such a situation, we considered the 1,8-triptycenediyl linker as a backbone whose folded structure would lessen repulsive interactions between the chelated anion and the bridgehead C-H unit. Using standard protocols, we generated the distibine **31** which was easily converted into the distiborane **32** (**Scheme 7**).[56] This compound readily complexes a fluoride anion *via* treatment with TBAT ` CH_2Cl_2 to form [**32**-F][TBA] (**Figure 11**).[56] Similar to [**30**-F]$^-$, a crystallographic analysis of this complex again shows the two Sb(V) centers clamping down on the bridging fluoride anion that is held by two short Sb-F bonds of 2.158(2) Å and 2.251(2) Å. Also, the Sb-Sb separation contracts from an average value of 5.203(11) Å in **31** to 4.3564(5) Å in **32**, allowing the Lewis acidic host to close down on its anionic guest.

Scheme 7. Oxidation of distibine 31 to distiborane 32 following treatment with 2 equivalents of *o*-chloranil.

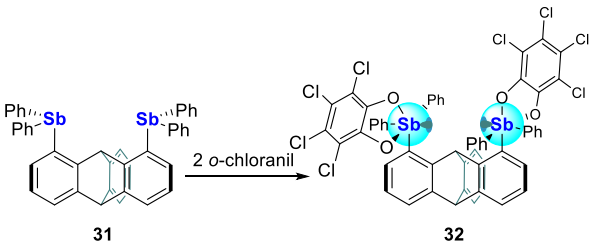

NBO analysis reveals the presence of a lp(F$^-$)→σ*($C_{bridgehead}$-H) donor-acceptor interaction of 5.9 kJ·mol^{-1} (**Figure 11**). Though weak, this C-H···F$^-$ bond is clearly observable by ^{1}H NMR spectroscopy. The triptycene derivative **32** also has a higher computed FIA value (395 kJ·mol^{-1}) than **30** (365 kJ·mol^{-1}), suggesting that it is more Lewis acidic than **30**. This computational result is corroborated by quantitative fluoride transfer from [**30**-F]$^-$ to **32** as confirmed by ^{19}F NMR spectroscopy (**Figure 11**).

Our work on these bidentate systems has also explored **33** and **34** two derivatives based on the *o*-phenylene backbones and featuring octafluorophenanthrene-9,10-diolate ligand on each antimony, as opposed to the *o*-tetrachlorocatecholate ligand found in **30** and

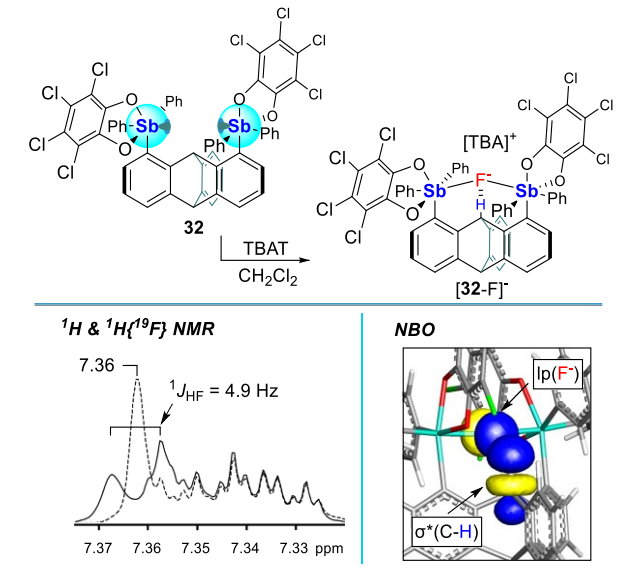

Figure 11. Top: Fluoride chelation by distiborane **32** upon treatment with TBAT in CH_2Cl_2. Bottom left: ^{1}H and ^{1}H{^{19}F} NMR showing the coupling of the bridgehead proton to the chelated fluoride in [**32**-F]$^-$. Bottom right: Representative NBO of the lp(F$^-$)→σ*(C-H) interaction at the triptycene bridgehead.

32 (**Scheme 8**),.[57] These compounds, which could be accessed using the corresponding distibines following oxidation with 9,10-perfluorophenanthraquinone, differ from one another *via* the nature of the *o*-phenylene backbone, which is perfluorinated in the case of **34**. Each readily complex fluoride upon addition of TBAT to form the corresponding anionic chelate complexes [**33**-F]$^-$ and [**34**-F]$^-$, respectively, as [TBA]$^+$ salts. In contrast to the roughly linear Sb-F-Sb vectors of [**30**-F]$^-$ (165.45(9)°) and [**32**-F]$^-$ (174.4(1)°), [**33**-F]$^-$ and [**34**-F]$^-$ display highly oblique Sb-F-Sb angles of 126.30(12)° and 129.48(6)°, respectively, reflecting the impact of the rigid *o*-phenylene backbone. Gas-phase FIA calculations suggest that **33** (391 kJ·mol^{-1}) and **34** (400 kJ·mol^{-1}) are among the most potent fluoride chelators that we have synthesized, with the higher Lewis acidity of **34** being assigned to the perfluorination of the *o*-phenylene backbone (**Figure 12**). The chelating binding motifs greatly enhances the FIA compared to the monofunctional **35** (FIA = 327 kJ·mol^{-1}), further confirming the efficacy of this strategy for anion binding.

Scheme 8. Fluoride chelation by 33 and 34 upon treatment with TBAT.

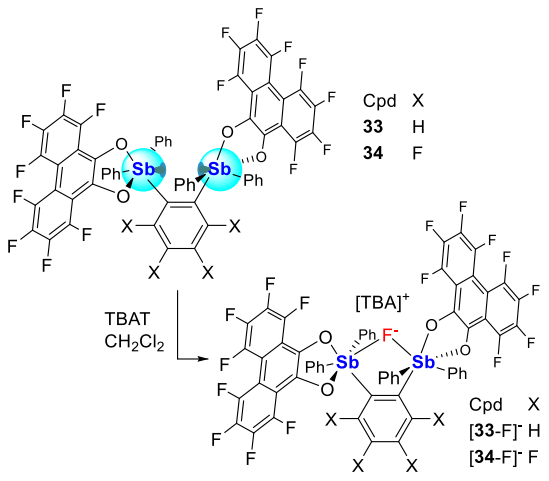

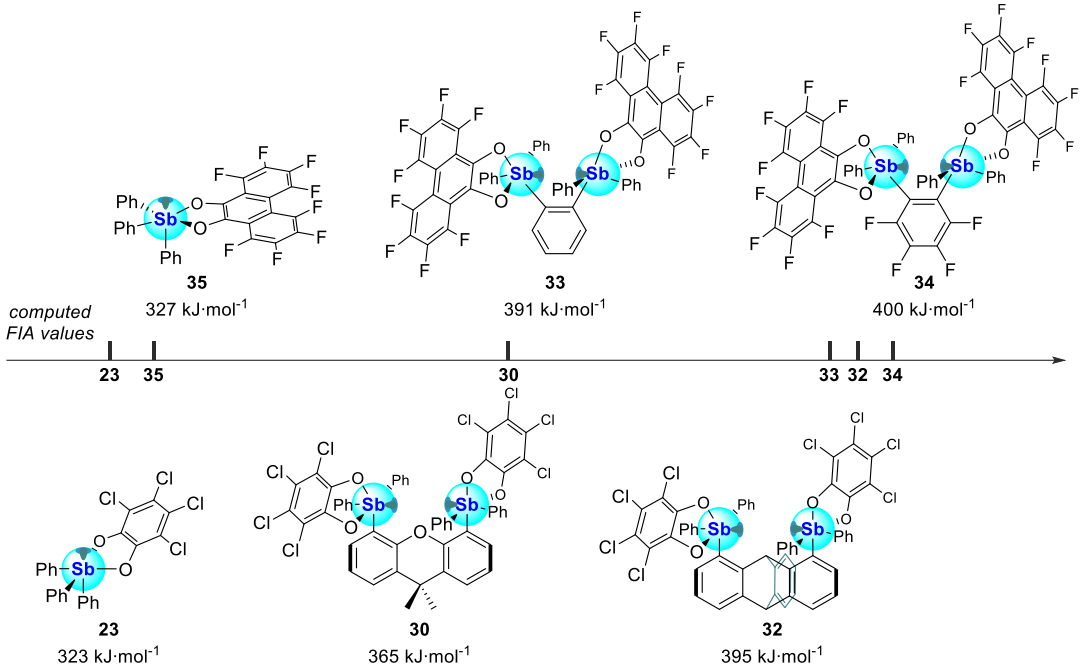

Figure 12. Schematic ranking of the computed gas-phase FIA values of monodentate and bidentate catecholatostiboranes based on gas-phase optimized geometries (level of theory: B3LYP/Sb: aug-cc-pVTZ-PP, Cl: 6-311G(d), F: 6-31G(d'), C/O/H: 6-31G).

Antimony (V) compounds – Stibonium cations

Tetraarylstibonium cations

Historical precedence has shown that the simplest tetraarylstibonium cation $[Ph_4Sb]^+$ ($[\mathbf{36}]^+$) favors the coordination of small, charge-dense anions[58] compared to larger anions.[59] Notably, $[\mathbf{36}]^+$ has long been known to extract aqueous fluoride under biphasic conditions.[13a, 60] Structural analyses of the halide salts of $[\mathbf{36}]^+$ indicate that the fluoride anion may be privileged for tight complexation by the Lewis acidic antimony center.[61] Indeed, the solid-state structure of **36**-F displays an Sb-F distance of 2.0530(8) Å,[58g] which slightly exceeds the sum of the covalent radii of the two elements ($R_{cov}(Sb) + R_{cov}(F) = 1.96$ Å).[62] However, as the halide (X) becomes heavier, the Sb-X bond length increasingly departs from its ideal covalent value, as indicated by the increasing formal shortness ratio (r = observed Sb-X bond length / ($R_{cov}(Sb) + R_{cov}(X)$), **Figure 13**).[63] This increase in r reflects greater ionicity of the Sb-X interaction.

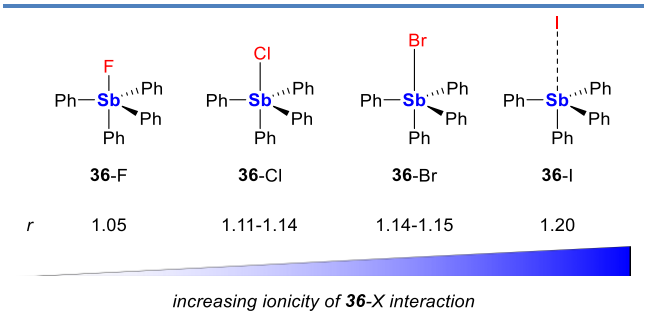

Figure 13. Structures of halide salts of $[\mathbf{36}]^+$ with Sb-X bonds that become increasingly ionic as depicted by their increasing formal shortness ratio (r) values. The r values were calculated from published metrical parameters for **36**-F,[58g] **36**-Cl,[58c, 64] **36**-Br,[58d, 59] and **36**-I.[61]

Our efforts to explore the upper limit of Lewis acidity in tetraarylstibonium cations has led us to consider perfluorinated derivatives.[65] Toward this end, we prepared $(C_6F_5)_4SbCl$ ($[\mathbf{37}$-Cl) by reaction of $SbCl_5$ with C_6F_5Li.[66] In line with the increased Lewis acidity imparted to the antimony center by the electron deficient aryl rings, **37**-Cl features an Sb-Cl bond of 2.4509(11) Å, which is much shorter than the values reported for **36**-Cl (2.6860(9) Å and 2.7395(10)).[58c, 64] The high Lewis acidity of $[\mathbf{37}]^+$, which was generated as a $[(C_6F_5)_4B]^-$ ($[BAr^F_4]^-$) salt using **37**-Cl and $[Et_3SiHSiEt_3][BAr^F_4]$, also manifests in its ability to abstract a fluoride anion from $[(C_6F_5)_3BF]^-$ and $[SbF_6]^-$ (**Scheme 9**), with the last reaction conferring it the distinction of a "Lewis superacid."[67] Interestingly, $[\mathbf{37}][SbCl_6]$, which can be easily generated from **37**-Cl and $SbCl_5$, exists as a stable salt thus highlighting how the antimony center of $[\mathbf{37}]^+$ privileges the smallest halide anion.[68]

Scheme 9. Fluoride complexation behavior of Lewis superacid $[\mathbf{37}]^+$.

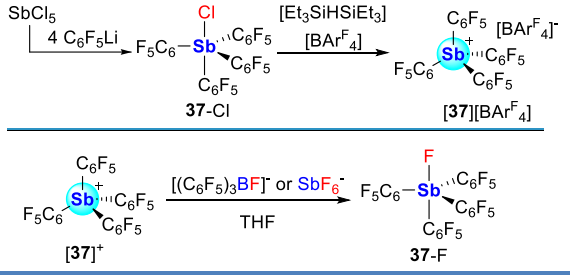

The anion complexation properties of tetraaryl stibonium centers persist even when near intramolecular Lewis bases.[69] Such is the case of $[\mathbf{38}]^+$ (**Figure 14**), which forms a strong intramolecular Lewis interaction with an *ortho* positioned phosphine oxide moiety

(Sb-O distance: 2.4315(13) Å).[70] Even if this interaction partially quenches the Lewis acidity compared to [**36**]$^+$, which by its ESP map has a deeper σ-hole than [**38**]$^+$, the latter readily binds fluoride in THF:water (8:2 (v/v)) with a $K(F^-)$ of 10,000 ± 1,000 M^{-1} by ^{31}P NMR spectroscopy.

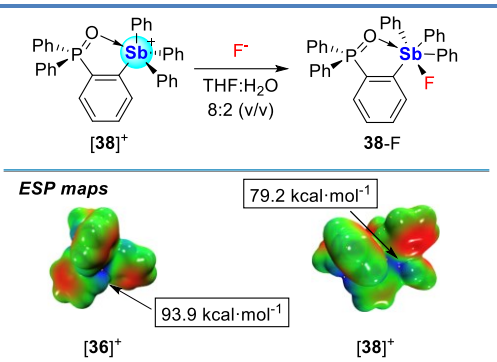

Figure 14. Top: Fluoride binding behavior of [**38**]$^+$ in THF:water (8:2 (v/v)). Bottom: ESP maps with arrows indicating the $V_{S,max}$ values of [**36**]$^+$ and [**38**]$^+$ (level of theory: B3LYP/Sb: cc-pVTZ with ECP28 MDF, P: 6-31+g(d), C/H/O 6-31g).

Placement of *o*-phenylthioether moieties on stiboniums [**39**]$^+$ and [**40**]$^+$ similarly result in somewhat passivating lp(S)→σ*(Sb-C) interactions.[71] However, because these donor-acceptor interactions are weak, these two cations, which were isolated as $[BF_4]^-$ salts, retain considerable Lewis acidity. Indeed, chloride titration experiments in MeCN monitored *via* UV-vis spectroscopy finds $K(Cl^-)$ values of 4,400 ± 100 M^{-1} and 2,340 ± 50 M^{-1} for [**39**]$^+$ and [**40**]$^+$, respectively (**Scheme 10**). These results suggest that the more electron-releasing *p*-tolyl substituents dampen the Lewis acidity of [**40**]$^+$ compared to [**39**]$^+$. Such a simple comparison serves as a reminder that the acceptor properties of the antimony center can be finely tuned by variation of its substituents.

Scheme 10. Chloride binding behavior of [39]$^+$ and [40]$^+$ in MeCN.

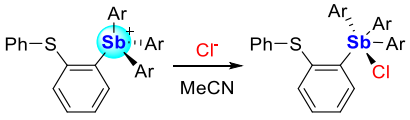

Cpd	Ar	$K(Cl^-)$
[**39**]$^+$	Ph	4,400 ± 100 M^{-1}
[**40**]$^+$	*p*-Tol	2,340 ± 50 M^{-1}

Positing that the Lewis acidity of the antimony center could be further elevated by alkylation of the thioether functionality, [**39**]$^+$ and [**40**]$^+$ were treated with $[Me_3O][BF_4]$, producing the sulfonium-stibonium dications [**41**]$^{2+}$ and [**42**]$^{2+}$. Both compounds display chloride anion binding constants in excess of 10^6 M^{-1} in MeCN (**Scheme 11**), which are several orders of magnitude higher than those of their monocationic precursors [**39**]$^+$ and [**40**]$^+$.[71] Computational studies show that the primarily antimony-bound chloride anion of [**41**-Cl]$^+$ and [**42**-Cl]$^+$ is stabilized by donor-acceptor bonding with the adjacent Lewis acidic sulfonium centers.[72] Thus, in addition to benefiting from enhanced Coulombic effects, chloride anion binding by [**41**]$^{2+}$ and [**42**]$^{2+}$ may also be enhanced by anion chelation.

Scheme 11. Top: Syntheses of [41]$^{2+}$ and [42]$^{2+}$ and chloride complexation.

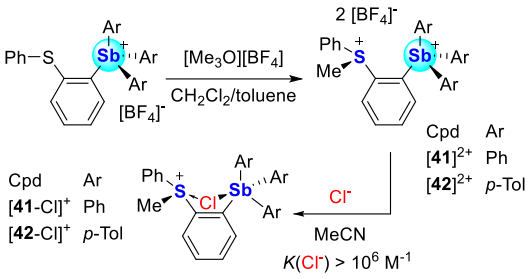

Triarylmethylstibonium cations

Lewis acidity is also evident in the chemistry of the $[MePh_3Sb]^+$ cation ([**43**]$^+$), which can be easily accessed by the quaternization of **13** with either MeOTf or $[Me_3O][BF_4]$ (**Figure 15**).[73] The solid-state structures of the $[OTf]^-$ and $[BF_4]^-$ salts of this cation display short contacts with their respective anions (Sb-O distance in [**43**][OTf]: 3.1518(17) Å;[73c] shortest Sb-F distance in [**43**][BF_4]: 3.189(10) Å[74]) speaking to the presence of a coordination site *trans* from a phenyl group. This coordination site readily engages a fluoride anion as confirmed by the isolation of **43**-F, which features an Sb-F bond of 2.0687(18) Å[75] similar to that found for **36**-F.

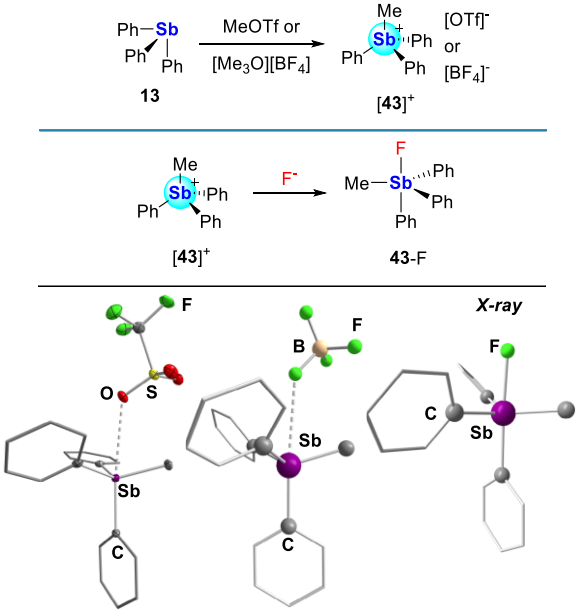

Figure 15. Top: Synthesis of [**43**]$^+$ by alkylation of **13** with either MeOTf or $[Me_3O][BF_4]$. Middle: Fluoride complexation by [**43**]$^+$. Bottom: Solid-state structures of [**43**][OTf] and [**43**][BF_4] depicting the short contacts formed between the stibonium centers and the counterions, as well as the solid-state structure of **43**-F. For [**43**][OTf],

Exploiting the simplicity by which triarylmethylstibonium cations can be synthesized, we prepared [**44**]$^{2+}$ as a simple bifunctional analogue and isolated this dication as a bis triflate salt ([**44**][$OTf]_2$, **Figure 16**).[73c] The crystal structure of this salt indicates that one of the triflate counterions bridges the two antimony centers, leading to Sb-O distances of 2.8541(12) Å and 2.9838(13) Å. These distances

are significantly shorter than that found in [**43**][OTf] (3.1518(17) Å), suggesting that the bidentate dication [**44**]$^{2+}$ is a more potent acceptor.

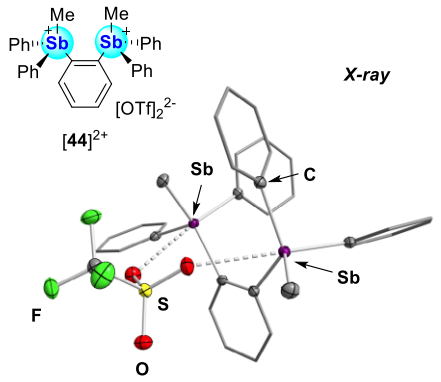

Figure 16. Structure of dicationic distibonium [**44**][OTf]$_2$. The solid-state structure of [**44**]$^{2+}$ depicting the chelation of an [OTf]$^-$ counterion across the two stibonium centers is also shown.

Anion chelation has also been unambiguously characterized in the case of the heteronuclear stibonium-borane cation [**46**]$^+$.[76] Indeed, this cation, which could be easily synthesized by reaction of the corresponding stibinoborane **45** with MeOTf (**Figure 17**), forms the corresponding fluoride complex **46**-F when treated with [TAS][Me_3SiF_2] (TASF). While the ^{19}F NMR chemical shift of this complex (-140.1 ppm) is in the range expected for a triarylfluoroborate species,[4c] its crystal structure shows that the fluoride anion bridges the two Lewis acids, resulting in a B-F bond of 1.521(4) Å and an Sb-F bond of 2.450(2) Å. A competition experiment involving [*o*-(Ph_2MeP)(Mes_2B-F)C_6H_4] (**47**-F),[77] the phosphorus analogue of **46**-F, shows quantitative transfer of the fluoride anion to [**46**]$^+$ in line with the greater Lewis acidity of the heavier pnictogen. The chelating properties of [**46**]$^+$ are also observed in the complexes that this cation forms with azide and cyanide anions.[78]

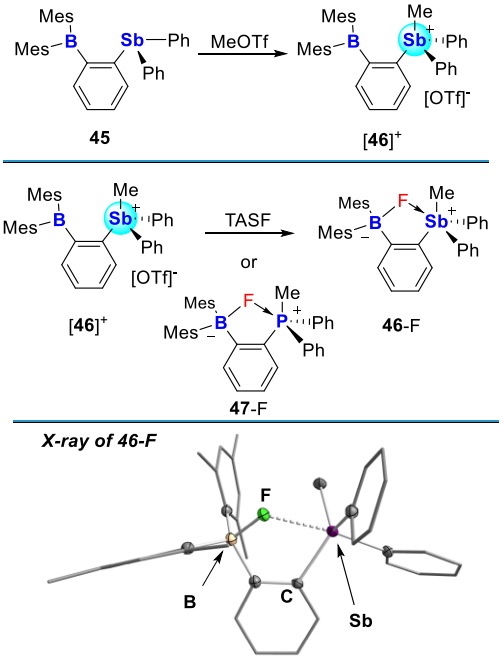

Figure 17. Top: Synthesis of stibonium-borane [**46**]$^+$ *via* alkylation of stibinoborane **45** with MeOTf. Middle: fluoride chelation by [**46**]$^+$ *via* TASF or *via* quantitative transfer from **47**-F. Bottom: Solid-state structure of **46**-F showing fluoride chelation between the borane and stibonium Lewis acidic centers.

Anion binding catalysis

Carbon-halide bond activation

Anion binding catalysis has emerged as a popular strategy for the activation of organic substrates whose electrophilic characteristics can be enhanced by cleavage of a carbon-halide (C-X) bond. This strategy has been successfully implemented using HB donor activators that engage the halide anion and promote the heterolytic dissociation of the C-X bond.[79] These advances have prompted the exploration of related approaches in which the HB donor activator is replaced by a main group Lewis acid such as a halogen-[80] or chalcogen-bond donor.[81] Though more limited, examples also exist where such reactions have involved PnB donors as activators. Matile and co-workers explored this possibility using stibines **3**, **4**, and **5**, which, as summarized earlier in **Figure 3**, display an affinity for the chloride anion that scales with the number of pentafluorophenyl groups.[36] The contrasting anion binding abilities of these compounds also inform their catalytic activities in reactions involving C-Cl bond activations. An example of such a reaction is provided by the activation of 1-chloroisochroman and the generation of an oxocarbenium intermediate that is readily intercepted by a ketene silyl acetal (**Figure 18**).[36] The yield of this reaction, after 55 h, increases in lockstep with the number of pentafluorophenyl groups on the stibine center, indicating the favorable influence played by the Lewis acidity of the pnictogen bond donor.

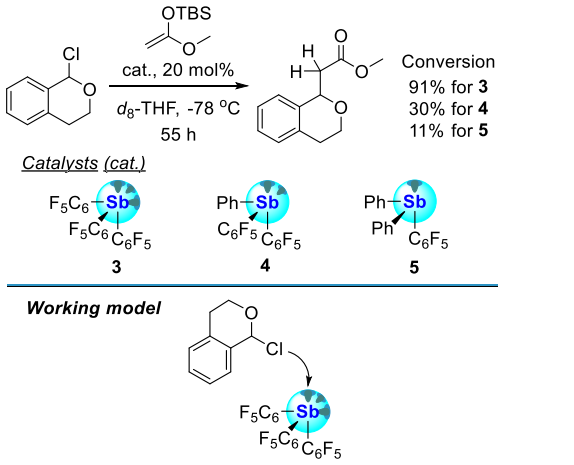

Figure 18. Top: Conversion of 1-chloroisochroman to methyl 2-(isochroman-1-yl)acetate *via* C-Cl activation by stibines **3**-**5**, with catalytic yields in line with the increasing Lewis acidity of the catalyst. Bottom: Working model of the catalysis facilitated by **3** depicting the heterolytic dissociation of the C-Br bond at the Lewis acidic stibine center.

Additional studies carried out in our laboratory have explored the role played by the redox state of the antimony center in the Ritter-type reaction of diphenylbromomethane (**Figure 19**).[19] This reaction, which necessitates activation of a C-Br bond, was investigated in CD_3CN at 40°C over the course of 24 h using stibine **12** and catecholatostiborane **25** as catalysts. While the reaction

proceeded with both catalysts, the conversion obtained with the antimony(V) derivative was markedly higher as indicated in **Figure 19**. These results are most simply rationalized by invoking the greater Lewis acidity of the oxidized antimony center of **25**. These results show that the redox state antimony atom provides another handle that can be adjusted to augment the catalytic properties of these compounds in reactions that proceed by an anion abstraction step.

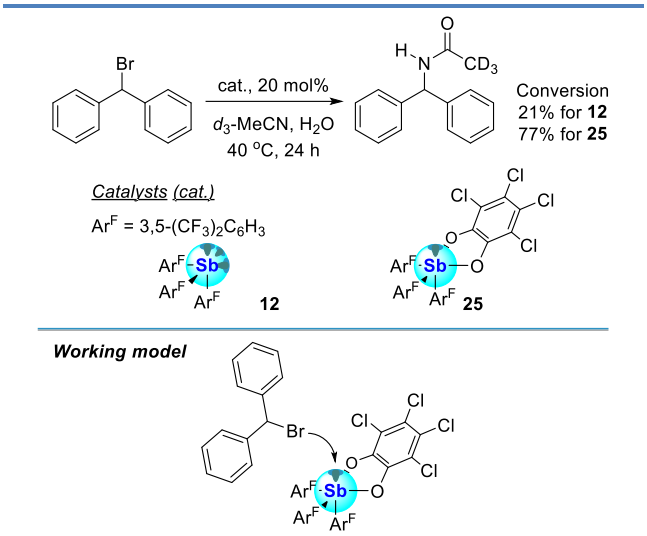

Figure 19. Top: Conversion of diphenylbromomethane to *N*-benzyhydrylacetamide in d_3-MeCN *via* C-Br activation by stibine **12** and catecholatostiborane **25**. Bottom: Working model of the catalysis facilitated by **25** depicting the heterolytic dissociation of the C-Br bond at the Lewis acidic catecholatostiborane center.

Metal-chloride bond activation

The Lewis acid-induced heterolysis of metal-halogen (M-X) bonds is a common strategy for the activation of transition metal catalysts.[82] While this method typically necessitates the use of strong Lewis acids such as fluorinated boranes, recent results have shown that the M-X bond of softer metals can be activated by hydrogen,[83] halogen[84] and chalcogen-bond donor functionalities.[85] One of our contributions to the development of such approaches has tested whether arylstibine dihalides may be sufficiently chloridophilic to activate M-Cl bonds for application in catalysis. To explore this question, we prepared **48**, a ligand containing a phosphine for metal coordination and a dichlorostibine unit as a chloridophilic PnB donor.[86] Auration with (tht)AuCl produced compound **48**-AuCl, allowing us to test the possibility of Au-Cl bond activation by the intramolecularly installed dichorostibine functionality upon addition of Ph_3P. This reaction produced the trichloroantimonate-containing zwitterion **49**, pointing to the ability of the dichorostibine moiety to participate in Au-Cl bond activation. This conclusion is also supported by the activity of **48**-AuCl as a catalyst for the cyclization of *N*-(prop-2-yn-1-yl)adamantine-1-carboxamide. This reaction, which produced the two isomers shown in **Figure 20**, proceeded to 87% conversion in 33 h when the reaction was carried out in CD_2Cl_2 with 2 mol% catalyst loading. For comparison, we also synthesized complex **50**-AuCl that features a much less potent PnB donor triarylantimony(III) unit and proved significantly less active than **48**-AuCl. These results support the proposal that the dichlorostibine moiety of **48** activates the gold center as depicted in the working model in **Figure 20**.

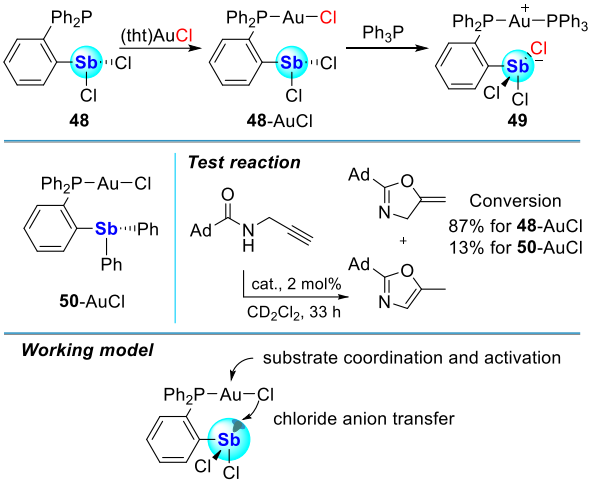

Figure 20. Top: Synthesis of **48**-AuCl *via* auration of **48**, and synthesis of **49** upon addition of Ph_3P to **48**-AuCl. Middle: Structure of **50**-AuCl, (left), and reaction used to compare the catalytic activities of **48**-AuCl and **50**-AuCl (right). Bottom: Working model developed to rationalize the activity of **48**-AuCl.

Anion sensing chemistry

Neutral platforms

As noted in the preceding sections, antimony derivatives display elevated anion affinities, leading us to question whether applications in anion sensing could be developed. Working toward this objective, we considered the case of chlorostibines such as Ph_2SbCl (**2**) that readily complex chloride anions to afford the corresponding $[Ph_2SbCl_2]^-$ ($[\mathbf{2}\text{-Cl}]^-$, **Scheme 2**). Positing that these simple anion binding events could form the basis of a halide recognition system, we decided to target a chlorostibine in which the antimony(III) atom is incorporated in a conjugated hydrocarbon π-system. Toward this end, we synthesized the stibaindole **51** as a bright yellow solid.[87] According to TD-DFT calculations (level of theory: MPW1PW91/Sb: aug-cc-pVTZ-pp, Cl: ECP10MWB, C/H: 6-31g(d)), this compound shows effective conjugation of the π* orbital of the conjugated hydrocarbon backbone and the σ*(Sb-Cl) orbital, which both end up contributing to the LUMO. This compound responds optically to the presence of halide anions including Cl^- in MeCN through the loss of its yellow color. This colorimetric response originates from the chloride-induced population of the σ*(Sb-Cl) orbital and the accompanying disruption of the aforementioned σ*/π* conjugation operative in the LUMO (**Figure 21**). In support of this interpretation, the solid-state structure of $[\mathbf{51}\text{-Cl}]^-$ shows that the chloride anion binds to the antimony center *trans* to the chloride ligand along a direction perpendicular to the stibaindole system. A titration experiment carried out in MeCN affords a chloride binding constant ($K(Cl^-)$) of 95,000 ± 5,000 M^{-1}. This elevated binding constant, which is comparable to that of $(C_6F_5)_3Sb$ (**3**),[36] speaks to the high Lewis acidity of **51**. This behavior contrasts with that of the phenyl analogue **52**, which shows no evidence of chloride binding under the same conditions. These diverging behaviors illustrate the determining role played by the chloride ligand in its ability to lower the energy of the antimony-centered LUMO while also deepening the corresponding σ-hole.

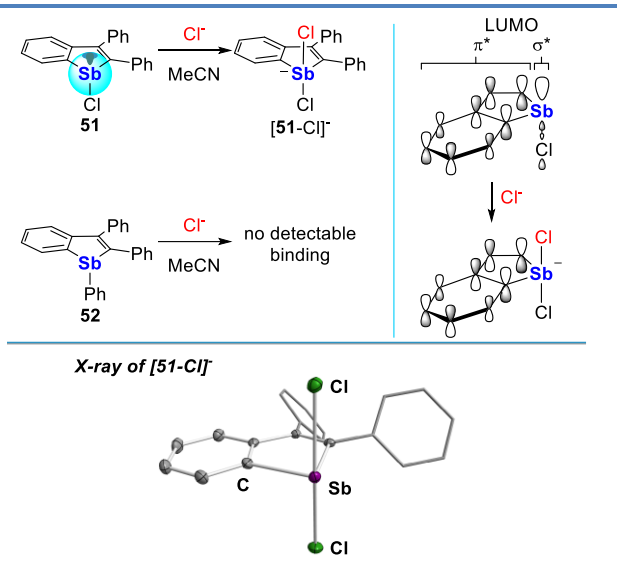

Figure 21. Top left: Chloride anion binding behavior by λ^3-stibaindoles **51** and **52** in MeCN. Top right: Idealized rendition of the origin of the response *via* chloride-induced disruption of the σ^*/π^* conjugation. Bottom: Solid-state structure of [**51**-Cl]$^-$.

Contemplating the possibility of anion sensing in aqueous environments and bearing in mind the high hydration energy that typifies anions such as fluoride, we have also investigated inherently more Lewis acidic antimony(V) compounds. With this in mind, we generated the bright yellow catecholatostiboranes **53** and **54** by oxidation of **52** with *o*-chloranil and 3,5-di-*tert*-butyl-*o*-benzoquinone, respectively (**Figure 22**).[88] The origin of their colors can be traced back to a stibaindole-based HOMO-1—LUMO transition, resulting in a UV-vis absorption band in the 340-350 nm range, which for both compounds tails into the visible. Interestingly, the stibaindole-based LUMO recruits considerable antimony character as a result of effective conjugation between the σ^*(Sb-C_{Ph}) orbital and the π^* orbital of the hydrocarbon backbone as in the case of **53** (**Figure 22**). Both **53** and **54** readily bind fluoride in chloroform and, in so doing, lose their bright yellow colors. This turn-off response arises from a disruption of the LUMO that no longer enjoys participation of the σ^*(Sb-C_{Ph}) orbital which is now monopolized for binding of the incoming fluoride anion. In THF:water solution (7:3 (v/v)), only **53** engages the fluoride anion, indicating that the more electron poor tetrachlorocatecholate is critical in engendering high Lewis acidity. *Via* DFT calculations (level of theory: B3LYP/Sb: aug-cc-pVTZ-pp, Cl: ECP10MWB, C/H/O: 6-31g(d)), we rationalized these differences as arising from a substantial lowering of the LUMO, which contains the Sb-C_{Ph} σ^* orbital, of **53** (-2.34 eV) compared to **54** (-1.84 eV). Finally, in a biphasic CH_2Cl_2-H_2O (pH 4.2, 10 mM citrate, 20 mM tetraisopropylammonium bromide) solution, **53** could selectively detect fluoride at levels below 1 ppm.

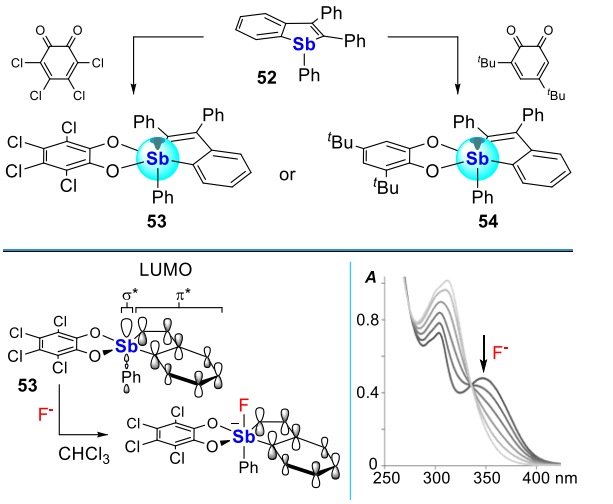

Figure 22. Top: Synthesis of $1\lambda^5$-stibaindoles **53** and **54** by oxidation of **52** with *ortho*-quinones. Bottom left: Idealized rendition of the origin of the response *via* fluoride binding-induced disruption of the σ^*/π^* conjugation at the LUMO. Bottom right: UV-vis spectra showing the response of **53** to fluoride binding in $CHCl_3$.

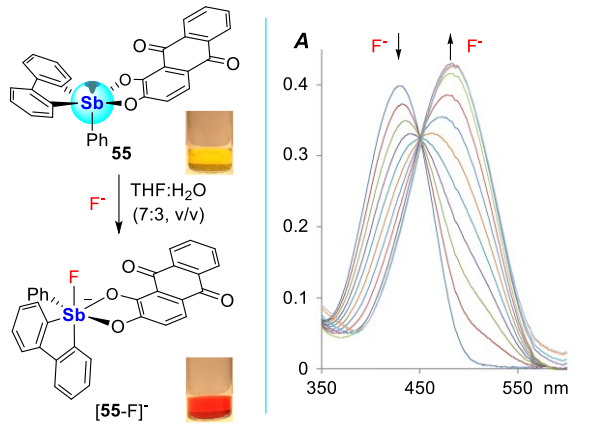

Figure 23. Left: Fluoride binding behavior of **55** in a THF:water (7:3 (v/v)) solution and colorimetric response to fluoride complexation in CH_2Cl_2. Right: UV-vis changes induced by fluoride complexation to **55** in CH_2Cl_2.

In another strategy, we considered analogs of the catecholatostiborane **27** (**Figure 8**), a compound that displays a high affinity for the fluoride anion in aqueous solutions but lacks any distinct photophysical response in the visible part of the spectrum.[53] Aiming to remediate this situation, we decided to replace the tetrachlorocatecholate ligand by a more performant chromophore such as alizarin,[89] which could be easily introduced into **55** using standard protocols (**Figure 23**).[53] Not only does **55** have a high $K(F^-)$ of 16,100 ± 1,100 M^{-1} in THF:water (7:3 (v/v)), fluoride binding induces a vibrant color change from yellow to orange (**Figure 23**). TD-DFT calculations (level of theory: B3LYP/ Sb: aug-cc-pVTZ-PP, F; 6-31g(d'), C/O/H: 6-31g) suggest that this color change is largely driven by an energy increase of the alizarin-based HOMO upon conversion of **55** into the more electron rich fluoroantimonate [**55**-F]$^-$. Moreover, an alizarin-based fluorescent turn-on response at 616 nm in dry CH_2Cl_2 is also seen between **55** (Φ_F = 0.2%) and [**55**-F]$^-$ (Φ_F = 3.0%), which is attributed to the increased rigidity of the fluoroantimonate (**Figure 23**). In a biphasic CH_2Cl_2-H_2O (pH 4.68, 10 mM citrate, 20 mM

tetrapropylammonium bromide) solution, fluoride binding was selective over Cl^-, Br^-, NO_3^-, HCO_3^-, $H_2PO_4^-$, and HSO_4^-, and was sensitive to fluoride at concentrations less than 1 ppm.

Cationic platforms

Our earlier work on cationic boron-based anion sensors revealed the determining influence that charge effects can exert over the anion binding at the boron center.[4c, 6] To build on these precedents, and encouraged by the demonstrated ability of $[Ph_4Sb]^+$ ($[\mathbf{36}]^+$) to sequester the fluoride anion under biphasic conditions,[13a, 60] we became eager to investigate the potential of stibonium cations as anion sensors. Since $[\mathbf{36}]^+$ lacks a read-out photophysical response, we replaced one of the phenyl groups by an anthryl group, leading to the isolation of $[\mathbf{56}]^+$ (**Figure 24**).[90] This water-

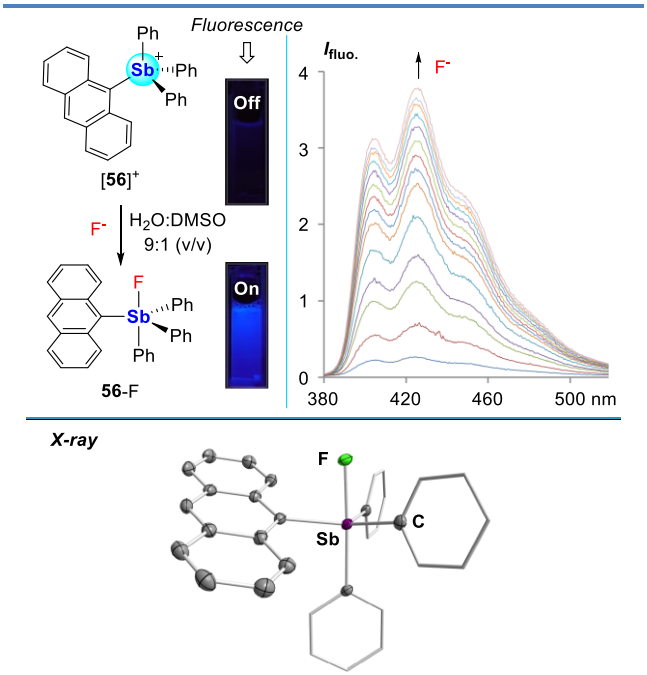

Figure 24. Top left: Fluoride binding behavior of $[\mathbf{56}]^+$ in water-DMSO (9:1 (v/v), pH 4.8, 10 mM pyridine, 10 mM cetyltrimethylammonium bromide), with the fluorescence response to fluoride binding visualized with a handheld UV lamp. Top right: Fluorescence response to fluoride binding. Bottom: Solid-state structure of **56**-F.

compatible stibonium cation is a potent Lewis acid. Because of competitive hydroxide binding, fluoride binding was studied in a water:DMSO (9:1 (v/v) solution buffered at pH 4.8 with pyridine (10 mM) in the presence of cetyltrimethylammonium bromide (10 mM). A UV-vis titration experiment carried out under these conditions afforded $K(F^-)$ = 12,000 ± 1,100 M^{-1}. To our surprise, fluoride binding to $[\mathbf{56}]^+$ elicited a fluorescence increase from Φ_F = 2.2% to Φ_F = 14.1% (**Figure 24**), enabling the use of this stibonium cation as a fluoride anion fluorescence turn-on sensor compatible with sub-ppm concentrations of the anion. Moreover, we found that this response was selective over other anions like Cl^-, and thus well adapted to fluoride sensing in tap and bottled water.

The mechanism of this fluorescence turn-on response was examined by Irle and co-workers *via* excited-state DFT calculations on $[\mathbf{56}]^+$ (level of theory: CAM-B3LYP/Sb: CRENBL, C: 6-311+G(d), H: 6-31G).[91] Two excited state minima were found in these calculations: an emissive bright state and a non-emissive dark state, that lies at lower energy. In the bright state, the antimony center retains its expected tetrahedral geometry with the HOMO and LUMO corresponding to the π and π* orbital of the anthryl ligand (**Figure 25**). The dark state is reached *via* a distortion of the antimony coordination geometry from tetrahedral to seesaw. This distortion, which lowers the energy of the excited state, also changes the nature of the frontier orbitals. The LUMO is particularly affected as it loses its anthryl π* character to locate on the antimony atom in the form of a σ*(Sb-C) orbital. This distorted excited state is non-emissive, presumably because of the relatively narrow separation between the two SOMOs. Donation of a fluoride lone

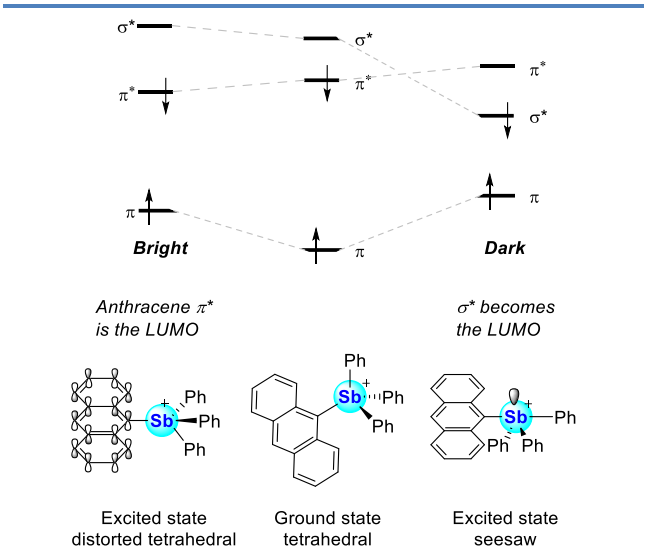

Figure 25. Schematic diagram of the geometry-induced orbital exchange responsible for the emissive properties of $[\mathbf{56}]^+$.

pair into the σ*(Sb-C) orbital prevents access to such a dark state in **56**-F thus restoring the π-π* emission of the anthracene chromophore. This mechanism also applies to other stibonium cations such as the pyrenyl and perylenyl systems $[\mathbf{57}]^+$ and $[\mathbf{58}]^+$,[92] and the BODIPY derivative $[\mathbf{59}]^+$ (**Figure 26**).[93] All three cations see their fluorescence readily increased upon fluoride binding at the antimony center. In the case of $[\mathbf{57}]^+$, this manifested in a fluorescence quantum yield increase from Φ_F = 0.5% to Φ_F = 5.2% upon fluoride binding.[92] A proportionally similar response is observed for $[\mathbf{58}]^+$, since fluoride binding elicits a fluorescence

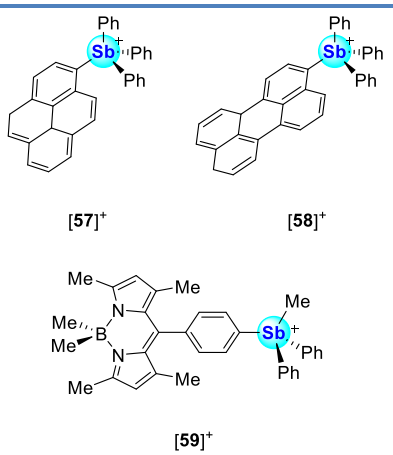

Figure 26. Structures of $[\mathbf{57}]^+$-$[\mathbf{59}]^+$, which undergo fluorescence turn-on responses to fluoride *via* a similar mechanism to $[\mathbf{56}]^+$.

increase from Φ_F = 7.3% to Φ_F = 59.2%. Like $[\mathbf{56}]^+$, $[\mathbf{57}]^+$ and $[\mathbf{58}]^+$

are potent fluoride binders with $K(F^-)$ values of 10,000 ± 800 M^{-1} and 10,000 ± 500 M^{-1} for $[\mathbf{57}]^+$ and $[\mathbf{58}]^+$ in a water:DMSO solution (9:1 (v/v), pH 4.8, 10 mM pyridine, 10 mM cetyltrimethylammonium bromide). The BODIPY derivative $[\mathbf{59}]^+$ could only be evaluated in MeCN, a medium in which itdisplays a $K(F^-)$ greater than 10^7 M^{-1} and a noticeable fluorescence turn-on response from Φ_F = 0.15 to Φ_F = 0.30 upon fluoride complexation.[93] DFT calculations (level of theory: B3LYP/Sb: aug-cc-pVTZ-PP, B/F: 6-31g(d'), C/H/N: 6-31g(d)) suggest that the turn-on response of $[\mathbf{59}]^+$ follows a similar mechanism to that of $[\mathbf{56}]^+$, with anion binding into the σ^*(Sb-$C_{phenylene}$) orbital rescuing the π-π^*-based emission of the BODIPY fluorophore.[88]

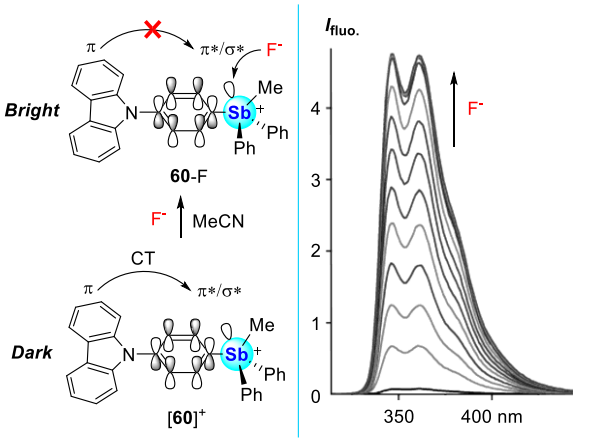

Figure 27. Left: Fluoride binding behavior of $[\mathbf{60}]^+$ in MeCN, with idealized rendition of the charge-transfer disruption upon fluoride binding. Right: Fluorescence response to fluoride binding in MeCN.

Aiming to replace the electron-poor BODIPY chromophore of $[\mathbf{59}]^+$ by an electron-rich one, we synthesized the carbazole derivative $[\mathbf{60}]^+$ and found it to be very weakly emissive (Φ_{PL} = 0.007 in MeCN) (**Figure 27**).[94] Addition of TBAF in MeCN affords a $K(F^-) > 10^7$ M^{-1}, and conversion to **60**-F elicits an order-of-magnitude increase in its quantum yield to Φ_{PL} of 0.060. Excited state DFT calculations (level of theory: CAM-B3LYP/Sb: aug-cc-pVTZ-PP with CRENBL ECP, C/H/N/F: 6-31+g(d')) found that this turn-on mechanism differs from that of $[\mathbf{56}]^+$. While the HOMO and LUMO of **60**-F are confined to the carbazole unit leading to an emissive π-to-π^* excited state, the LUMO of $[\mathbf{60}]^+$ resides on the antimony-decorated phenylene unit displaying mixed σ^*(Sb-C)/π^* character. It follows that in the case of $[\mathbf{60}]^+$, the classical carbazole-centered π-to-π^* excited state is replaced by an excited state resulting from charge-transfer from the carbazole-based HOMO to the above mentioned σ^*(Sb-C)/π^* orbital. Experimentally, this excited state is very weakly emissive, possibly because of a narrowed HOMO-LUMO gap.

Transmembrane anion transport by antimony compounds

Beyond the realms of catalysis and optical sensing, anion recognition is also essential to myriad biological processes. Chief among these processes is the selective transport of anions across hydrophobic membranes, which is typically facilitated by cell membrane-embedded proteins that form a selective channel to allow for the passage of anions. In so-called channelopathic diseases,[95] defects in the structure or the expression of these proteins disrupt homeostatic anion transport. Perhaps the best known of these diseases is cystic fibrosis, wherein mutations of the CFTR chloride-bicarbonate anion channel dysregulate its transport activity, leading to a range of harmful consequences.[96] Investigation into small-molecule treatments for channelopathies has been spent developing "carrier-type" anion transporters that are typically water stable, lipophilic, and adorned with a HB donor binding pocket. These structural attributes allow these transporters to capture anions on one side of a membrane, shuttle through the membrane, and deposit the anion on the other side.[97]

The parallels existing between HB-based anion transporters and organoantimony anion binders discussed previously have led our group and that of Matile to test whether electron deficient stibines and stibonium cations could also promote anion transport across phospholipid bilayers via a carrier-type mechanism such as that depicted in **Figure 28**.[98] As such, the transport activities of $Ph(C_6F_5)_2Sb$ (**4**) were assessed in egg yolk phosphatidylcholine (EYPC) large unilamellar vesicles (LUVs) loaded with the ratiometric pH probe 8-hydropyrene-1,3,6-trisulfonic acid (HPTS) and a buffered solution of NaCl (**Figure 29**).[99] Upon

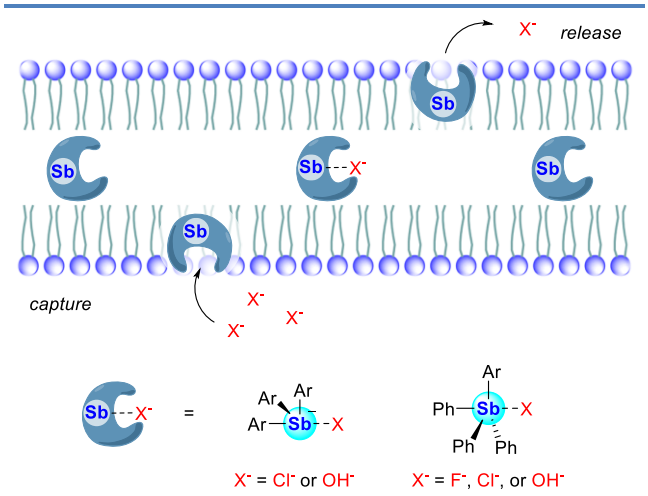

Figure 28. Antimony-based Lewis acids transporting anions across a phospholipid bilayer membrane *via* a carrier-type mechanism.

administration of a base pulse to the external solution in which the LUVs are suspended followed by administration of **4**, rapid dissipation of the pH gradient was exhibited via Cl^-/OH^- exchange, as indicated by changes in the HPTS fluorescence spectrum.

The EC_{50} value of this transporter, equal to the concentration of the transporter needed to reach 50% chloride transport after 5 min, was estimated to be 1 μM, suggesting that this compound is indeed very active.[99] This study also established that $(C_6F_5)_3Sb$ (**3**) does not behave ideally as it also triggers lysis of the vesicles, leading to release of the anionic cargo. A subsequent study also indicated that this molecule is not water stable.[100] These stability limitations do not seem to affect $(3,4,5\text{-}C_6F_3H_2)_3Sb$ (**8**) and $(2,4,6\text{-}C_6F_3H_2)_3Sb$ (**61**), which were also evaluated using the above mentioned HPTS assay.[100] Remarkably, while **61** showed an activity that is moderately improved when compared to that of **4** (EC_{50} = 0.27 ± 0.02 μM for **61** *vs.* 1 μM for **4**), compound **8** displays a much higher activity as indicated by its EC_{50} value of 2.6 ± 0.8 nM, which is three orders of magnitude lower than that of **4**. While no explanation for this

significant increase between **4** and **8** is provided, it was suggested that **61** is penalized by the *ortho*-fluorine substituents that may hinder the anion binding site or donate to the antimony atom, thereby reducing its Lewis acidity or pnictogen bond donor ability.

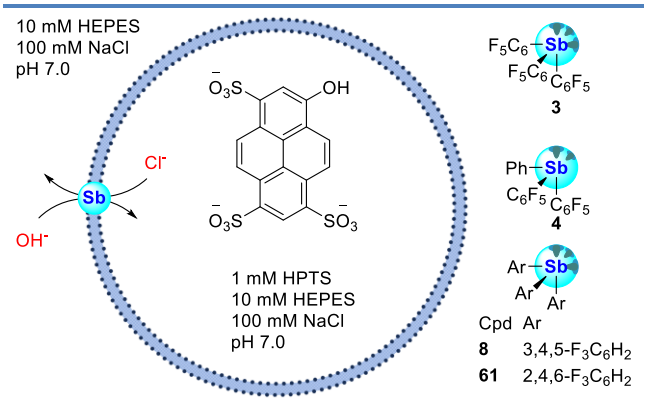

Figure 29. Simplified illustration of the HPTS assay as employed by Matile using EYPC LUVs depicting Cl^-/OH^- antiport upon administration of a base pulse. The structures of stibines **3**, **4**, **8**, and **61** used as transporters are also shown.

Concomitant with the above efforts, we investigated the anion transport properties of stibonium cations.[101] These studies, which were encouraged by the known ability of triarylphosphonium cations to permeate through biological membranes,[102] first focused on tetraarylstibonium cations that were already known to promote anion phase transfer while also serving as water compatible anion sensors.[13a, 60, 90, 92] We first evaluated $[\mathbf{36}]^+$, $[\mathbf{56}]^+$, $[\mathbf{57}]^+$, $[\mathbf{62}]^+$ and using a fluoride ion selective electrode (ISE) and EYPC LUVs loaded with KF (**Figure 30**).[101] We found all four compounds to be potent transporters, either *via* an F^-/OH^- antiport mechanism or *via* KF efflux when administered in the presence of valinomycin as a potassium ion transporter (**Figure 30**). While all four cations are potent transporters, we observed that the activity of $[\mathbf{56}]^+$ and $[\mathbf{57}]^+$ far exceed those of the other two cations considered, namely $[\mathbf{36}]^+$ and $[\mathbf{62}]^+$. These observations led us to propose that the lipophilic character of the stibonium structure assists in partitioning the transporter into the membrane, thus leading to more potent transport. This is supported by computed *n*-octanol/water partition coefficient calculations ($\log K_{ow}$), which showed that $[\mathbf{56}]^+$ and $[\mathbf{57}]^+$ were at least an order of magnitude more lipophilic ($\log K_{ow}$ values of 5.85 and 6.26, respectively) than the lower performing $[\mathbf{36}]^+$ and $[\mathbf{62}]^+$ ($\log K_{ow}$ values of 4.19 and 5.09, respectively). Transport data collected with $[\mathbf{56}]^+$ and $[\mathbf{57}]^+$ in the presence of valinomycin afforded EC_{50} values at 270 s of 0.41 ± 0.05 mol% and 0.57 ± 0.07 mol% , respectively. These EC_{50} values indicate that $[\mathbf{56}]^+$ and $[\mathbf{57}]^+$ rival the transport properties of strapped calix[4]pyrroles investigated *via* fluoride ISE in 1-palmitoyl-2-oleoyl-*sn*-glycero-3-phosphocholine (POPC) vesicles by Gale and co-workers.[103] We will also note that these values are

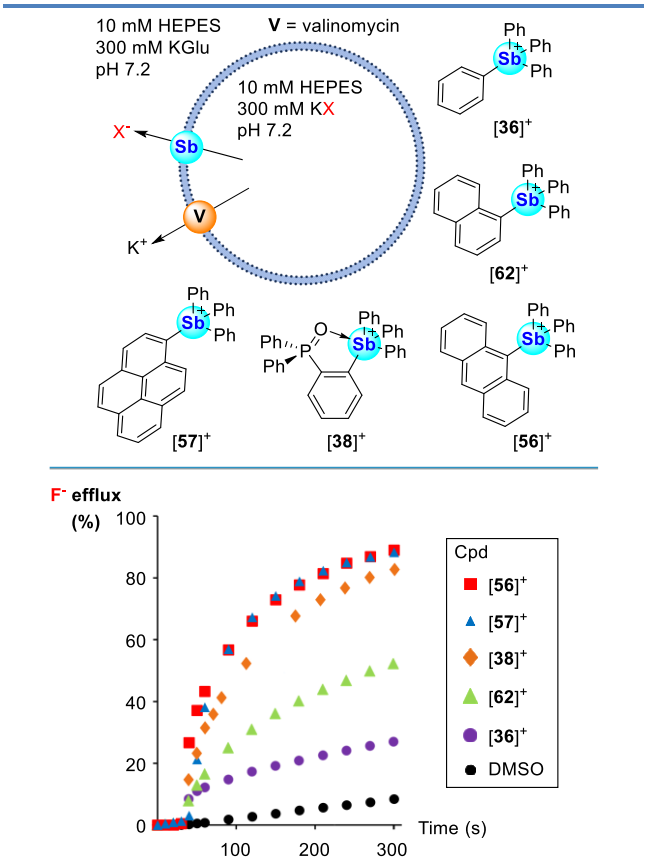

Figure 30. Top: Simplified illustration of the ISE assay as employed by our group using EYPC and POPC LUVs depicting potassium halide salt efflux upon administration of valinomycin and a stibonium cation as transporter. The structures of stibonium cations $[\mathbf{36}]^+$, $[\mathbf{62}]^+$, $[\mathbf{56}]^+$, $[\mathbf{57}]^+$, and $[\mathbf{38}]^+$ used as transporters are also shown. Bottom: Fluoride efflux profiles comparing the transport activities of stibonium cations $[\mathbf{36}]^+$, $[\mathbf{56}]^+$, $[\mathbf{57}]^+$, $[\mathbf{62}]^+$ (in EYPC LUVs), and $[\mathbf{38}]^+$ (in POPC LUVs) added as DMSO solutions, in the presence of valinomycin.

close to those measured for phosphonium boranes,[104] which we have also used as fluoride anion transporters. The observation of fluoride transport in the absence of valinomycin provided initial evidence that these stibonium cations may also transport hydroxide anions. We confirmed this possibility using $[\mathbf{36}]^+$, which was deployed in an HPTS assay using EYPC vesicles. This conclusion is reinforced by a recent study employing a lanthanide-based selectivefluoride sensor immobilized inside POPC vesicles to assess fluoride influx.[105] Using different fluorescence assays, this study concluded, that under the experimental conditions, $[\mathbf{56}]^+$ is indeed a potent hydroxide anion transporter. It follows that $[\mathbf{56}]^+$ may also induce acidification of the vesicle interior and thus formation of HF ($pK_a = 3.17$) that can diffuse spontaneously through the membrane. This possibility serves as a reminder that studying the transport of basic anions such as fluoride is inherently complicated.

The fluoride transport properties of stibonium cations do not seem to be affected by the intramolecular coordination of a donor group to the antimony center. Such is the case for the aforementioned $[\mathbf{38}]^+$ whose gas phase FIA is damped by intramolecular coordination of a phosphine oxide compared to the parent $[\mathbf{36}]^+$ (125.0 kcal·mol^{-1} and 133.0 kcal·mol^{-1}, respectively).[70] Nevertheless, this cation is a very effective transporter, as evidenced by its ability to transport fluoride across the membranes of POPC LUVs (**Figure 30**). The EC_{50} value of 0.24 ± 0.03 mol% shows that its potency is on par with $[\mathbf{56}]^+$, leading us to propose that the high

lipophilicity of $[\mathbf{38}]^+$ (log K_{ow} = 7.20) plays a determining role in its performance. These results demonstrate that the transport properties of these stibonium cations survive the introduction of a Lewis basic ligand, providing another dimension along which the composition, properties, and possible conjugability of the transporter could be adjusted.

Along similar lines, we observed that the *o*-phenylthioether-stibonium cation $[\mathbf{40}]^+$ is also a very potent anion transporter, as indicated by an assay that employed POPC LUVs loaded with KCl (**Figure 31**).[71] Indeed, the EC_{50} of this compound was found to be 0.63 ± 0.03 mol%. The elevated activity of this transporter is correlated to the Lewis acidity of antimony center as well as the overall lipophilicity of the structure (log K_{ow} = 7.68), which promotes recruitment of the transporter to the hydrophobic part of the membrane. As part of this study, we also assayed its corresponding sulfonium-stibonium dication $[\mathbf{42}]^{2+}$. Even though it is substantially more chloridophilic than $[\mathbf{40}]^+$, $[\mathbf{42}]^{2+}$ is a significantly less effective transporter. The lower performance of this species is assigned to its decreased lipophilicity (log K_{ow} = 1.26), which probably severely limits its ability to partition into the membrane. The contrasting properties of these two compounds led to the hypothesis that the $[\mathbf{40}]^+/[\mathbf{42}]^{2+}$ pair could serve as the basis for a stimulus-responsive transport system that can be activated under specific conditions or in a specific biological environment. With this idea in mind, we decided to investigate whether $[\mathbf{42}]^{2+}$ may undergo reduction of the sulfonium center and thus convert into the much more active $[\mathbf{40}]^+$, when in a reductive environment This possibility was tested using glutathione (GSH), which we first verified cleanly reduces $[\mathbf{42}]^{2+}$ into $[\mathbf{40}]^+$, in aqueous solutions (D_2O:d_6-DMSO, 7.9:2.1 (v/v), pH 7.6, 300 mM sodium phosphate) by ^{1}H NMR spectroscopy. We also confirmed that addition of GSH to a solution of KCl-loaded POPC vesicles pretreated with $[\mathbf{42}]^{2+}$ followed by incubation leads to increased chloride efflux upon administration of valinomycin, as a result of the *in situ* conversion of $[\mathbf{42}]^{2+}$ into the more active $[\mathbf{40}]^+$. Increasing the concentration of GSH showed a positive correlation with the extent of transport activation, adding further credence to our interpretation (**Figure 31**).[71]

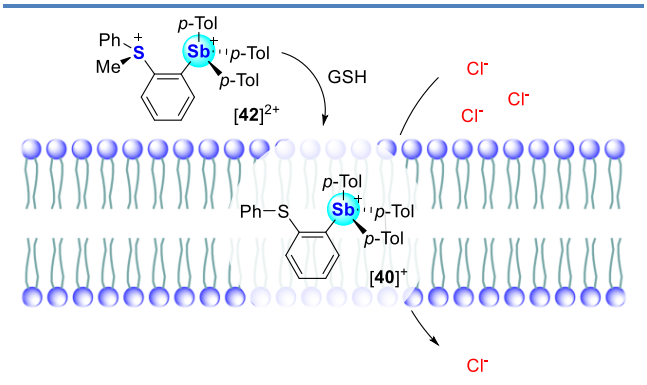

Figure 31. Reductive demethylation of pre-transporter $[\mathbf{42}]^{2+}$ with GSH to yield active chloride transporter $[\mathbf{40}]^+$.

Finally, with the view of testing stibonium-based anion transporters in biological settings, we decided to test their ability to accelerate the known toxicity of fluoride toward human red blood cells (RBCs), causing oxidative stress and hemolysis when in the presence of fluoride.[106] Using this toxic side effect as a marker of anion transport, we compared the rate of hemolysis of a sample of RBCs in fluoridated media (100 μM) and $[\mathbf{56}]^+$ (5 μM).[101] The extent of hemolysis was monitored over time, reaching 48% after 8 h. By comparison, incubation of the RBCs in fluoridated media alone induced only 17% hemolysis after 8 h, while the transporter $[\mathbf{56}]^+$ in the absence of fluoride was found to be non-toxic. The accelerated fluoride-induced toxicity observed in the presence $[\mathbf{56}]^+$ suggests that the stibonium cation facilitates transport of the fluoride anions inside the RBCs (**Figure 32**).

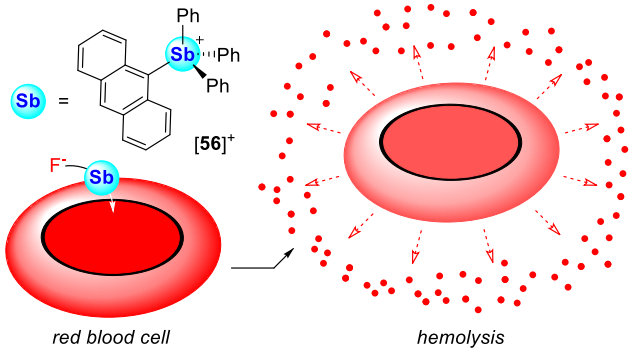

Figure 32. Illustration of the fluoride-induced hemolysis of red blood cells facilitated by fluoride influx by transporter $[\mathbf{56}]^+$.

Conclusions and Outlook

The chemistry of organoantimony derivatives has long been limited to structural studies. Over the course of several decades these studies have revealed the Lewis acidic tendencies that antimony display especially when bearing electron-withdrawing ligands or when in the pentavalent state. Recent efforts aimed at reclassifying the natural Lewis acidity of antimony derivatives as its ability to form pnictogens bond, or in other words *dative bonds*, with donors have continued to mostly focus on deciphering the structure of the resulting adducts and the nature of the bond connecting the antimony center to the donor. Strikingly, until about fifteen years ago, very few efforts had been made to translate the natural Lewis acidity of organoantimony species into a functional context. Our work from the past twelve years, and the contributions of other groups, has begun to change this state of affair with the demonstration that the Lewis acidity of these main group derivates derivatives can be purposefully exploited for application in anion sensing, anion binding catalysis, and anion transport. The results presented in this Perspective, which focus on our contribution to this area, underscore several important facets, including the ease of synthesis of Lewis acidic organoantimony compounds, their stability toward ambient and aqueous conditions, and the facile tunability of their Lewis acidity, that enable application in aqueous chemistry where the antimony center is not irreversibly neutralized by water. These group 15 Lewis acids, whose tunability is reminiscent of that of boron-based systems, surpass their group 13 analogs in such conditions, raising the prospect for a bright future in the chemistry of organoantimony derivatives as Lewis acids, or synonymously pnictogen bond donors.

Thus, the results presented in this Perspective serve as a prelude for antimony's bright future, specifically in the context of anion binding chemistry. The diverse structural variations that can be implemented to augment anion binding and the simple strategies

that can be used to encode photophysical responses provide initial evidence of future possibilities in the field of anion sensing. The same is true in the domain of anion transport chemistry where stibonium cations have found a new niche as potent carriers of biologically relevant anions across phospholipid membranes. We note though that a deeper understanding of the anion selectivity of these transporters is imperative given that a target anion will constantly compete with hydroxide binding at biological pH values. Attention should also be paid towards expanding the structural breadth of these compounds such that they can toggle their Lewis acidic properties. Clearly the lipophilic character of the transporter influences its anionophoric activity, but the influence of other biological triggers on transporter structure remains to be determined.

Finally, returning to the fundamental aspects that underpin this chemistry, we will note that while extremely useful, the σ hole concept is limited in terms of its ability to predict how anion binding to an antimony center may alter the electronic features of the entire platform. Such a limitation is made particularly obvious by our work on anion sensing, where orbital and electronic structure analyses are necessary to explain the various colorimetric and fluorescence responses we have observed. Thus, we recommend that the σ hole and the σ* orbital models always be paired when considering such chemistry.

AUTHOR INFORMATION

Corresponding Author

François P. Gabbaï – Department of Chemistry, Texas A&M University, College Station, Texas 77843, United States. orcid.org/0000-0003-4788-2998. Email: francois@tamu.edu

Author

Brendan L. Murphy – Department of Chemistry, Texas A&M University, College Station, Texas 77843, United States.

Notes

There are no conflicts to declare.

Acknowledgements

This work was performed at Texas A&M University with support of the National Science Foundation (CHE-2108728), the Welch Foundation (A-1423), and Texas A&M University (Arthur E. Martell Chair of Chemistry). B.L.M gratefully acknowledges support from the National Science Foundation (NSF-GRFP, DGE-2139772).

REFERENCES

1. (a) Piers, W. E.; Chivers, T., Pentafluorophenylboranes: from obscurity to applications. *Chem. Soc. Rev.* **1997,** *26,* 345-354; (b) Erker, G., Tris(pentafluorophenyl)borane: a special boron Lewis acid for special reactions. *Dalton Trans.* **2005**, 1883-1890.
2. (a) Piers, W. E.; Marwitz, A. J. V.; Mercier, L. G., Mechanistic Aspects of Bond Activation with Perfluoroarylboranes. *Inorg. Chem.* **2011,** *50,* 12252-12262; (b) Stephan, D. W.; Erker, G., Frustrated Lewis Pair Chemistry: Development and Perspectives. *Angew. Chem. Int. Ed.* **2015,** *54,* 6400-6441.
3. Lee, M. H.; Agou, T.; Kobayashi, J.; Kawashima, T.; Gabbaï, F. P., Fluoride ion complexation by a cationic borane in aqueous solution. *Chem. Commun.* **2007**, 1133-1135.
4. (a) Agou, T.; Sekine, M.; Kobayashi, J.; Kawashima, T., Detection of Biologically Important Anions in Aqueous Media by Dicationic Azaborines Bearing Ammonio or Phosphonio Groups. *Chem. Eur. J.* **2009,** *15,* 5056-5062; (b) Wade, C. R.; Broomsgrove, A. E. J.; Aldridge, S.; Gabbaï, F. P., Fluoride Ion Complexation and Sensing Using Organoboron Compounds. *Chem. Rev.* **2010,** *110,* 3958-3984; (c) Hudnall, T. W.; Chiu, C.-W.; Gabbaï, F. P., Fluoride ion recognition by chelating and cationic boranes. *Acc. Chem. Res.* **2009,** *42,* 388-397.
5. Chiu, C.-W.; Kim, Y.; Gabbaï, F. P., Lewis Acidity Enhancement of Triarylboranes via Peripheral Decoration with Cationic Groups. *J. Am. Chem. Soc.* **2009,** *131,* 60-61.
6. Zhao, H.; Leamer, L. A.; Gabbaï, F. P., Anion capture and sensing with cationic boranes: on the synergy of Coulombic effects and onium ion-centred Lewis acidity. *Dalton Trans.* **2013,** *42,* 8164-8178.
7. Hudnall, T. W.; Gabbaï, F. P., Ammonium Boranes for the Selective Complexation of Cyanide or Fluoride Ions in Water. *J. Am. Chem. Soc.* **2007,** *129,* 11978-11986.
8. Lippert, A. R.; Van de Bittner, G. C.; Chang, C. J., Boronate oxidation as a bioorthogonal reaction approach for studying the chemistry of hydrogen peroxide in living systems. *Acc. Chem. Res.* **2011,** *44,* 793-804.
9. Gutmann, V.; Hubacek, H.; Steininger, A., Color indicators in proton-free solutions. III. Crystal Violet in phosphorus oxychloride. *Monatsh. Chem.* **1964,** *95,* 678-686.
10. (a) Olah, G. A.; Kuhn, S. J.; Tolgyesi, W. S.; Baker, E. B., Stable Carbonium Ions. II.1a Oxocarbonium1b (Acylium) Tetrafluoroborates, Hexafluorophosphates, Hexafluoroantimonates and Hexafluoroarsenates. Structure and Chemical Reactivity of Acyl Fluoride: Lewis Acid Fluoride Complexes1c. *J. Am. Chem. Soc.* **1962,** *84,* 2733-2740; (b) Olah, G. A.; Tolgyesi, W. S.; Kuhn, S. J.; Moffatt, M. E.; Bastien, I. J.; Baker, E. B., Stable carbonium ions. IV. Secondary and tertiary alkyl and aralkyl oxocarbonium hexafluoroantimonates. Formation and identification of the trimethylcarbonium ion by decarbonylation of the tert-butyl oxocarbonium ion. *J. Am. Chem. Soc.* **1963,** *85,* 1328-34; (c) Olah, G. A.; Baker, E. B.; Evans, J. C.; Tolgyesi, W. S.; McIntyre, J. S.; Bastien, I. J., Stable carbonium ions. V. Alkylcarbonium hexafluoroantimonates. *J. Am. Chem. Soc.* **1964,** *86,* 1360-73.
11. (a) Calves, J. Y.; Gillespie, R. J., The methyl fluoride-antimony pentafluoride and arsenic pentafluoride systems: the formation of methyl fluoride.antimony pentafluoride and methyl fluoride.arsenic pentafluoride and the methylation of thionyl fluoride and sulfuryl chloride fluoride. *J. Am. Chem. Soc.* **1977,** *99,* 1788-1792; (b) Bacon, J.; Gillespie, R. J., Methyl and Ethyl Hexafluoroantimonate and Related Compounds. *J. Am. Chem. Soc.* **1971,** *93,* 6914-6919.
12. Olah, G. A.; Prakash, G. K. S.; Molnár, Á.; Sommer, J. *Superacid chemistry,* 2nd ed.; Wiley: Hoboken, NJ, 2009.
13. (a) Moffett, K. D.; Simmler, J. R.; Potratz, H. A., Solubilities of Tetraphenylstibonium Salts of Inorganic Anions. Procedure For Solvent Extraction of Fluoride Ion From Aqueous Medium. *Anal. Chem.* **1956,** *28,* 1356-1356; (b) Hall, M.; Sowerby, D. B., Synthesis and crystal structure of bis(triphenylantimony catecholate) hydrate. A new square-pyramidal antimony(V) compound. *J. Am. Chem. Soc.* **1980,** *102,* 628-632.
14. (a) Lin, T.-P.; Wade, C. R.; Pérez, L. M.; Gabbaï, F. P., A Mercury→Antimony Interaction. *Angew. Chem. Int. Ed.* **2010,** *49,* 6357-6360; (b) Wade, C. R.; Lin, T.-P.; Nelson, R. C.; Mader, E. A.; Miller, J. T.; Gabbaï, F. P., Synthesis, structure and properties of a T-shaped 14-electron stiboranyl-gold complex. *J. Am. Chem. Soc.* **2011,** *133,* 8948-8955; (c) You, D.; Gabbaï, F. P., Unmasking the Catalytic Activity of a Platinum Complex with a Lewis Acidic, Non-innocent Antimony Ligand. *J. Am. Chem. Soc.* **2017,** *139,* 6843-6846.
15. (a) Wade, C. R.; Ke, I.-S.; Gabbaï, F. P., Sensing of Aqueous Fluoride Anions by Cationic Stibine–Palladium Complexes. *Angew. Chem. Int. Ed.* **2012,** *51,* 478-481; (b) Ke, I.-S.; Jones, J. S.; Gabbaï, F. P., Anion-Controlled Switching of an X Ligand into a Z Ligand: Coordination Non-innocence of a Stiboranyl Ligand. *Angew. Chem. Int. Ed.* **2014,** *53,* 2633-2637.
16. Baaz, M.; Gutmann, V.; Kunze, O., Die Chloridionenaffinitäten von Akzeptorchloriden in Acetonitril, 1. Mitt.: Lösungszustand und Bildungsgleichgewichte der Triphenylchlormethankomplexe. *Monatsh. Chem.* **1962,** *93,* 1142-1161.

17. van Zeist, W.-J.; Bickelhaupt, F. M., The activation strain model of chemical reactivity. *Org. Biomol. Chem.* **2010,** *8,* 3118-3127.
18. de Azevedo Santos, L.; Hamlin, T. A.; Ramalho, T. C.; Bickelhaupt, F. M., The pnictogen bond: a quantitative molecular orbital picture. *Phys. Chem. Chem. Phys.* **2021,** *23,* 13842-13852.
19. Yang, M.; Tofan, D.; Chen, C.-H.; Jack, K. M.; Gabbaï, F. P., Digging the Sigma-Hole of Organoantimony Lewis Acids by Oxidation. *Angew. Chem. Int. Ed.* **2018,** *57,* 13868-13872.
20. (a) Erdmann, P.; Leitner, J.; Schwarz, J.; Greb, L., An Extensive Set of Accurate Fluoride Ion Affinities for p-Block Element Lewis Acids and Basic Design Principles for Strong Fluoride Ion Acceptors. *ChemPhysChem* **2020,** *21,* 987-994; (b) Krossing, I.; Raabe, I., Relative stabilities of weakly coordinating anions: A computational study. *Chem. Eur. J.* **2004,** *10,* 5017-5030; (c) Moc, J.; Morokuma, K., Ab initio MO study on the periodic trends in structures and energies of hypervalent compounds: five-, six-, and seven-coordinated XF_5, XH_6^-, XF_6^-, XH_7^{2-} and XF_7^{2-} species containing a group 15 central atom (where X is P, As, Sb, Bi). *J. Mol. Struct.* **1997,** *436-437,* 401-418; (d) Christe, K. O.; Dixon, D. A.; McLemore, D.; Wilson, W. W.; Sheehy, J. A.; Boatz, J. A., On a quantitative scale for Lewis acidity and recent progress in polynitrogen chemistry. *J. Fluorine Chem.* **2000,** *101,* 151-153.
21. Maltz, L. T.; Gabbaï, F. P., Analyzing Fluoride Binding by Group 15 Lewis Acids: Pnictogen Bonding in the Pentavalent State. *Inorg. Chem.* **2023,** *accepted,* doi:10.1021/acs.inorgchem.3c01987.
22. Varadwaj, A.; Varadwaj, P. R.; Marques, H. M.; Yamashita, K., Definition of the Pnictogen Bond: A Perspective. *Inorganics* **2022,** *10,* 149.
23. Cavallo, G.; Metrangolo, P.; Milani, R.; Pilati, T.; Priimagi, A.; Resnati, G.; Terraneo, G., The Halogen Bond. *Chem. Rev.* **2016,** *116,* 2478-2601.
24. Wang, W.; Ji, B.; Zhang, Y., Chalcogen bond: a sister noncovalent bond to halogen bond. *J. Phys. Chem. A* **2009,** *113,* 8132-5.
25. Bauzá, A.; Mooibroek, T. J.; Frontera, A., The Bright Future of Unconventional σ/π-Hole Interactions. *ChemPhysChem* **2015,** *16,* 2496-2517.
26. Alcock, N. W., Secondary Bonding to Nonmetallic Elements. In *Advances in Inorganic Chemistry and Radiochemistry,* Emeléus, H. J.; Sharpe, A. G., Eds. Academic Press: 1972; Vol. 15, pp 1-58.
27. Norman, N. C., Coordination Chemistry of Antimony and Bismuth: Lewis Acidity,σ* -Orbitals and Coordination Geometry. *Phosphorus, Sulfur, and Silicon and the Related Elements* **1994,** *87,* 167-176.
28. Scheiner, S., A new noncovalent force: Comparison of P···N interaction with hydrogen and halogen bonds. *J. Chem. Phys.* **2011,** *134,* 094315.
29. (a) Himmel, D.; Krossing, I.; Schnepf, A., Dative Bonds in Main-Group Compounds: A Case for Fewer Arrows! *Angew. Chem. Int. Ed.* **2014,** *53,* 370-374; (b) Haaland, A., Covalent versus Dative Bonds to Main Group Metals, a Useful Distinction. *Angew. Chem. Int. Ed.* **1989,** *28,* 992-1007; (c) Zhao, L.; Hermann, M.; Holzmann, N.; Frenking, G., Dative bonding in main group compounds. *Coord. Chem. Rev.* **2017,** *344,* 163-204.
30. Mundt, O.; Becker, G.; Stadelmann, H.; Thurn, H., Element—Element-Bindungen. VII. Intermolekulare Wechselwirkungen bei Dihalogen(phenyl)stibanen. *Z. Anorg. Allg. Chem.* **1992,** *617,* 59-71.
31. (a) Hall, M.; Sowerby, D. B., Phenylchloroantimon(III)ates; their preparations, and the crystal structures of $Me_4N[PhSbCl_3]$, $[Hpy]_2[PhSbCl_4]$, and $Me_4N[Ph_2SbCl_2]$. *J. Organomet. Chem.* **1988,** *347,* 59-70; (b) Preut, H.; Huber, F.; Alonzo, G., 1H^+,1'H^+-2,2'-Bipyridinium di-μ-chloro-bis[dichloro(phenyl)antimonate(III)]. *Acta Crystallogr., Sect. C: Cryst. Struct. Commun.* **1987,** *43,* 46-48.
32. (a) Carmalt, C. J.; Cowley, A. H.; Culp, R. D.; Jones, R. A.; Kamepalli, S.; Norman, N. C., Synthesis and Structures of Intramolecularly Base-Coordinated Group 15 Aryl Halides. *Inorg. Chem.* **1997,** *36,* 2770-2776; (b) Burford, N.; Macdonald, C. L. B.; LeBlanc, D. J.; Cameron, T. S., Synthesis and Characterization of Bis(2,4,6-tri(trifluoromethyl)phenyl) Derivatives of Arsenic and Antimony: X-ray Crystal Structures of $As(R_F)_2Cl$, $Sb(R_F)_2Cl$, abd $Sb(R_F)_2OSO_2CF_3$. *Organometallics* **2000,** *19,* 152-155; (c) Artali, R.; Bombieri, G.; Bertazzi, N., Tetramethylammonium chlorodiphenylthiocyanatoantimonate(III). *Acta Crystallogr E* **2005,** *61,* M2733-M2735; (d) Sharma, D.; Balasubramaniam, S.; Kumar, S.; Jemmis, E. D.; Venugopal, A., Reversing Lewis acidity from bismuth to antimony. *Chem. Commun.* **2021,** *57,* 8889-8892; (e) Sharma, D.; Benny, A.; Gupta, R.; Jemmis, E. D.; Venugopal, A., Crystallographic evidence for a continuum and reversal of roles in primary–secondary interactions in antimony Lewis acids: applications in carbonyl activation. *Chem. Commun.* **2022,** *58,* 11009-11012.
33. Becker, G.; Mundt, O.; Sachs, M.; Breunig, H. J.; Lork, E.; Probst, J.; Silvestru, A., Element-element bonds. X. Studies of chloro(diphenyl)stibane, tribenzylstibane and tribenzyldibromostiborane - Molecular structures and isotypism. *Z. Anorg. Allg. Chem.* **2001,** *627,* 699-714.
34. Calderazzo, F.; Marchetti, F.; Ungari, F.; Wieber, M., Reactivity of Molecules Containing Element-Element Bonds. 3. Reduction of Halo-Organometallics of Antimony(III) and Bismuth(III) - Crystal and Molecular-Structure of $CoCp_2[SbPh_2Cl_2]$. *Gazz. Chim. Ital.* **1991,** *121,* 93-100.
35. (a) Levason, W.; McAuliffe, C. A., Coordination chemistry of organostibines. *Acc. Chem. Res.* **1978,** *11,* 363-8; (b) Levason, W.; Reid, G., Developments in the coordination chemistry of stibine ligands. *Coord. Chem. Rev.* **2006,** *250,* 2565-2594.
36. Benz, S.; Poblador-Bahamonde, A. I.; Low-Ders, N.; Matile, S., Catalysis with pnictogen, chalcogen, and halogen bonds. *Angew. Chem. Int. Ed.* **2018,** *57,* 5408-5412.
37. Kuhn, H.; Docker, A.; Beer, P. D., Anion Recognition with Antimony(III) and Bismuth(III) Triaryl-Based Pnictogen Bonding Receptors. *Chem-Eur J* **2022,** *28,* e202201838.
38. (a) Qiu, J.; Unruh, D. K.; Cozzolino, A. F., Design, Synthesis, and Structural Characterization of a Bisantimony(III) Compound for Anion Binding and the Density Functional Theory Evaluation of Halide Binding through Antimony Secondary Bonding Interactions. *J. Phys. Chem. A* **2016,** *120,* 9257-9269; (b) Qiu, J.; Song, B.; Li, X.; Cozzolino, A. F., Solution and gas phase evidence of anion binding through the secondary bonding interactions of a bidentate bis-antimony(III) anion receptor. *Phys. Chem. Chem. Phys.* **2018,** *20,* 46-50.
39. Qiu, J.; Bateman, C. N.; Lu, S.; George, G. C., III; Li, X.; Gorden, J. D.; Vasylevskyi, S.; Cozzolino, A. F., Solution Studies of a Water-Stable, Trivalent Antimony Pnictogen Bonding Anion Receptor with High Binding Affinities for CN–, OCN–, and OAc–. *Inorg. Chem.* **2023,** *62,* 12582-12589.
40. Zaitseva, E. G.; Medvedev, S. V.; Aslanov, L. A., Crystal and Molecular-Structures of Cesium Phenylpentachloroantimonate $Cs[PhSbCl_5]$, Potassium Phenylpentabromoantimonate $K[PhSbBr_5]$, and Cesium Hexachloroantimonate $Cs[SbCl_6]$. *J. Struct. Chem.* **1990,** *31,* 92-97.
41. (a) Nunn, M.; Begley, M. J.; Sowerby, D. B.; Haiduc, I., Complexes of organoantimony(III) and (V) halides with nitrogen donors. *Polyhedron* **1996,** *15,* 3167-3174; (b) Breunig, H. J.; Koehne, T.; Moldovan, O.; Preda, A. M.; Silvestru, A.; Silvestru, C.; Varga, R. A.; Piedra-Garza, L. F.; Kortz, U., Syntheses, structures and intermolecular interactions of tetraorganoammonium, -phosphonium and -stibonium dimethyl- and diphenyltetrahaloantimonates. *J. Organomet. Chem.* **2010,** *695,* 1307-1313.
42. Karimi, M.; Gabbaï, F. P., Hydrogen Bond-Assisted Fluoride Binding by a Stiborane. *Z. Anorg. Allg. Chem.* **2022,** e202200098.
43. Kasemann, R.; Naumann, D., Tieftemperatur-flüssigphasefluorierung von pentafluorphenyl-element-Verbindungen. Darstellungen und eigenschaften von $(C_6F_5)_3AsF_2$, $(C_6F_5)_3SbF_2$, $(C_6F_5)_2SeF_2$, $(C_6F_5)_2SeO$, $C_6F_5TeF_3$ und $Cs[(C_6F_5)_3EF_3]$ (E = As, Sb) [1]. *J. Fluorine Chem.* **1988,** *41,* 321-334.
44. Kojima, S.; Doi, Y.; Okuda, M.; Akiba, K. Y., First Stereochemical Characterization of Configurationally Stable Diastereomers of Hypervalent Stiboranes (10-Sb-5) and Acceleration of Intramolecular Permutation by Donor Solvents. *Organometallics* **1995,** *14,* 1928-1937.
45. Holmes, R. R.; Day, R. O.; Chandrasekhar, V.; Holmes, J. M., Pentacoordinated Molecules .67. Formation and Structure of Cyclic 5-Coordinated Antimony Derivatives - the 1st Square-Pyramidal Geometry for a Bicyclic Stiborane. *Inorg. Chem.* **1987,** *26,* 157-163.
46. Hirai, M.; Gabbaï, F. P., Squeezing Fluoride out of Water with a Neutral Bidentate Antimony(V) Lewis Acid. *Angew. Chem. Int. Ed.* **2015,** *54,* 1205-1209.

47. Krüger, G. J.; Pistorius, C. W. F. T.; Heyns, A. M., Potassium hexafluoroantimonate (I). *Acta Crystallogr., Sect. B: Struct. Sci* **1976,** *32,* 2916-2918.
48. Gini, A.; Paraja, M.; Galmés, B.; Besnard, C.; Poblador-Bahamonde, A. I.; Sakai, N.; Frontera, A.; Matile, S., Pnictogen-bonding catalysis: brevetoxin-type polyether cyclizations. *Chem. Sci.* **2020,** *11,* 7086-7091.
49. Chishiro, A.; Akioka, I.; Sumida, A.; Oka, K.; Tohnai, N.; Yumura, T.; Imoto, H.; Naka, K., Tetrachlorocatecholates of triarylarsines as a novel class of Lewis acids. *Dalton Trans.* **2022,** *51,* 13716-13724.
50. (a) Liberman-Martin, A. L.; Bergman, R. G.; Tilley, T. D., Lewis Acidity of Bis(perfluorocatecholato)silane: Aldehyde Hydrosilylation Catalyzed by a Neutral Silicon Compound. *J. Am. Chem. Soc.* **2015,** *137,* 5328-5331; (b) Thorwart, T.; Roth, D.; Greb, L., Bis(pertrifluoromethylcatecholato)silane: Extreme Lewis Acidity Broadens the Catalytic Portfolio of Silicon. *Chem. Eur. J.* **2021,** *27,* 10422-10427; (c) Hartmann, D.; Schädler, M.; Greb, L., Bis(catecholato)silanes: assessing, rationalizing and increasing silicon's Lewis superacidity. *Chem. Sci.* **2019,** *10,* 7379-7388; (d) Maskey, R.; Schädler, M.; Legler, C.; Greb, L., Bis(perchlorocatecholato)silane—A Neutral Silicon Lewis Super Acid. *Angew. Chem. Int. Ed.* **2018,** *57,* 1717-1720.
51. Roth, D.; Wadepohl, H.; Greb, L., Bis(perchlorocatecholato)germane: Hard and Soft Lewis Superacid with Unlimited Water Stability. *Angew. Chem. Int. Ed.* **2020,** *59,* 20930-20934.
52. Roth, D.; Stirn, J.; Stephan, D. W.; Greb, L., Lewis Superacidic Catecholato Phosphonium Ions: Phosphorus–Ligand Cooperative C–H Bond Activation. *J. Am. Chem. Soc.* **2021,** *143,* 15845-15851.
53. Hirai, M.; Gabbaï, F. P., Lewis acidic stiborafluorenes for the fluorescence turn-on sensing of fluoride in drinking water at ppm concentrations. *Chem. Sci.* **2014,** *5,* 1886-1893.
54. Smith, J. E.; Gabbaï, F. P., Are Ar_3SbCl_2 Species Lewis Acidic? Exploration of the Concept and Pnictogen Bond Catalysis Using a Geometrically Constrained Example. *Organometallics* **2023,** *42,* 240-245.
55. (a) Katz, H. E., Recent advances in multidentate anion complexation. *Inclusion Compd.* **1991,** *4,* 391-405; (b) Hawthorne, M. F.; Zheng, Z., Recognition of Electron-Donating Guests by Carborane-Supported Multidentate Macrocyclic Lewis Acid Hosts: Mercuracarborand Chemistry. *Acc. Chem. Res.* **1997,** *30,* 267-276; (c) Hoefelmeyer, J. D.; Schulte, M.; Tschinkl, M.; Gabbaï, F. P., Naphthalene derivatives peri-substituted by Group 13 elements. *Coord. Chem. Rev.* **2002,** *235,* 93-103.
56. Chen, C.-H.; Gabbaï, F. P., Fluoride Anion Complexation by a Triptycene-Based Distiborane: Taking Advantage of a Weak but Observable C−H···F Interaction. *Angew. Chem. Int. Ed.* **2017,** *56,* 1799-1804.
57. You, D.; Zhou, B.; Hirai, M.; Gabbaï, F. P., Distiboranes based on *ortho*-phenylene backbones as bidentate Lewis acids for fluoride anion chelation. *Org. Biomol. Chem.* **2021,** *19,* 4949-4957.
58. (a) Beauchamp, A. L.; Bennett, M. J.; Cotton, F. A., Molecular structure of tetraphenylantimony hydroxide. *J. Am. Chem. Soc.* **1969,** *91,* 297-301; (b) Ferguson, G.; Hawley, D. M., Crystal and molecular structure of micro -carbonato-bis(tetraphenylantimony). System containing penta- and hexacoordinated antimony. *Acta Crystallogr., Sect. B: Struct. Crystallogr. Cryst. Chem.* **1974,** *30,* 103-11; (c) Lebedev, V. A.; Bochkova, R. I.; Kuz'min, E. A.; Sharutin, V. V.; Belov, N. V., Crystal structure of $C_{24}H_{20}ClSb$. *Dokl. Akad. Nauk SSSR* **1981,** *260,* 1124-1127; (d) Knop, O.; Vincent, B. R.; Cameron, T. S., Pentacoordination and ionic character: crystal structure of bromotetraphenylantimony, Ph_4SbBr. *Can. J. Chem.* **1989,** *67,* 63-70; (e) Arvanitis, G. M.; Berardini, M. E.; Acton, T. B.; Dumas, P. E., Synthesis of two tetraphenylantimony complexes of pyridine N-oxides: crystal structure of tetraphenylantimony (2-mercaptopyridine N-oxide). *Phosphorus, Sulfur Silicon Relat. Elem.* **1993,** *82,* 127-135; (f) Haiges, R.; Schroer, T.; Yousuffudin, M.; Christe, K. O., The syntheses and structures of Ph_4EN_3 (E = P, As, Sb), an example for the transition from ionic to covalent azides within the same main group. *Z. Anorg. Allg. Chem.* **2005,** *631,* 2691-2695; (g) Sharutin, V. V.; Sharutina, O. K.; Pakusina, A. P.; Smirnova, S. A.; Pushilin, M. A., The structure of tetraarylantimony halides and tetraphenylantimony isothiocyanate. *Russ. J. Coord. Chem.* **2005,** *31,* 108-114; (h) Robertson, A. P. M.; Chitnis, S. S.; Jenkins, H. A.; McDonald, R.; Ferguson, M. J.; Burford, N., Establishing the Coordination Chemistry of Antimony(V) Cations: Systematic Assessment of $Ph_4Sb(OTf)$ and $Ph_3Sb(OTf)_2$ as Lewis Acceptors. *Chem. Eur. J.* **2015,** *21,* 7902-7913.
59. Ferguson, G.; Glidewell, C.; Lloyd, D.; Metcalfe, S., Effect of the counter ion on the structures of tetraphenylantimony(V)-stibonium compounds: crystal and molecular structures of tetraphenylantimony(V) bromide, perchlorate, and tetraphenylborate. *J. Chem. Soc., Perkin Trans. 2* **1988**, 731-735.
60. (a) Bowen, L. H.; Rood, R. T., Solvent extraction of ^{18}F as tetraphenylstibonium fluoride. *J. Inorg. Nucl. Chem.* **1966,** *28,* 1985-1990; (b) Jean, M., Tetraphenylstibonium fluoride. Ultraviolet measurements. *Anal. Chim. Acta* **1971,** *57,* 438-439.
61. Baker, L.-J.; Rickard, C. E. F.; Taylor, M. J., Structural investigations of the organoantimony(V) halides Ph_4SbX and Ph_3SbX_2 (X = Cl, Br or I) in the solid state and in solution. *Dalton Trans.* **1995**, 2895-2899.
62. Cordero, B.; Gomez, V.; Platero-Prats, A. E.; Reves, M.; Echeverria, J.; Cremades, E.; Barragan, F.; Alvarez, S., Covalent radii revisited. *Dalton Trans.* **2008**, 2832-2838.
63. Cotton, F. A., Discovering and understanding multiple metal-to-metal bonds. *Acc. Chem. Res.* **2002,** *11,* 225-232.
64. Sharutin, V. V.; Sharutina, O. K.; Pakusina, A. P.; Platonova, T. P.; Zadachina, O. P.; Gerasimenko, A. V., Phenylation of antimony(V) organic compounds with pentaphenylantimony. The structure of tetraphenylantimony chloride. *Russ. J. Coord. Chem.* **2003,** *29,* 89-92.
65. (a) Coughlin, O.; Krämer, T.; Benjamin, S. L., Cationic Triarylchlorostibonium Lewis Acids. *Organometallics* **2023,** *42,* 339-346; (b) García-Monforte, M. A.; Alonso, P. J.; Ara, I.; Menjón, B.; Romero, P., Solid-State and Solution Structure of a Hypervalent AX_5 Compound: $Sb(C_6F_5)_5$. *Angew. Chem. Int. Ed.* **2012,** *51,* 2754-2757.
66. Pan, B.; Gabbaï, F. P., $[Sb(C_6F_5)_4][B(C_6F_5)_4]$: An Air Stable, Lewis Acidic Stibonium Salt That Activates Strong Element-Fluorine Bonds. *J. Am. Chem. Soc.* **2014,** *136,* 9564-9567.
67. Greb, L., Lewis Superacids: Classifications, Candidates, and Applications. *Chem. Eur. J.* **2018,** *24,* 17881-17896.
68. Yang, M.; Pati, N.; Belanger-Chabot, G.; Hirai, M.; Gabbaï, F. P., Influence of the catalyst structure in the cycloaddition of isocyanates to oxiranes promoted by tetraarylstibonium cations. *Dalton Trans.* **2018,** *47,* 11843-11850.
69. Arias-Ugarte, R.; Devarajan, D.; Mushinski, R. M.; Hudnall, T. W., Antimony(V) cations for the selective catalytic transformation of aldehydes into symmetric ethers, α,β-unsaturated aldehydes, and 1,3,5-trioxanes. *Dalton Trans.* **2016,** *45,* 11150-11161.
70. Gonzalez, V. M.; Park, G.; Yang, M.; Gabbaï, F. P., Fluoride anion complexation and transport using a stibonium cation stabilized by an intramolecular P=O → Sb pnictogen bond. *Dalton Trans.* **2021,** *50,* 17897-17900.
71. Park, G.; Gabbaï, F. P., Redox-controlled chalcogen and pnictogen bonding: the case of a sulfonium/stibonium dication as a preanionophore for chloride anion transport. *Chem. Sci.* **2020,** *11,* 10107-10112.
72. (a) Kim, Y.; Gabbaï, F. P., Cationic Boranes for the Complexation of Fluoride Ions in Water below the 4 ppm Maximum Contaminant Level. *J. Am. Chem. Soc.* **2009,** *131,* 3363-3369; (b) Kim, Y.; Kim, M.; Gabbaï, F. P., Synthesis and Anion Affinity of a Bidendate Sulfonium Fluorosilane Lewis Acid. *Org. Lett.* **2010,** *12,* 600-602; (c) Zhao, H.; Kim, Y.; Park, G.; Gabbaï, F. P., Controlling the fluoridophilicity of sulfonium boranes via chelation, Coulombic and hydrophobic effects. *Tetrahedron* **2019,** *75,* 1123-1129.
73. (a) Henry, M. C.; Wittig, G., The Organometallic Alkylidene Reaction. *J. Am. Chem. Soc.* **1960,** *82,* 563-564; (b) McCortney, B. A.; Jacobson, B. M.; Vreeke, M.; Lewis, E. S., Methyl transfers. 14. Nucleophilic catalysis of nucleophilic substitution. *J. Am. Chem. Soc.* **1990,** *112,* 3554-3559; (c) Hirai, M.; Cho, J.; Gabbaï, F. P., Promoting the Hydrosilylation of Benzaldehyde by Using a Dicationic Antimony-Based Lewis Acid: Evidence for the Double Electrophilic Activation of the Carbonyl Substrate. *Chem. Eur. J.* **2016,** *22,* 6537-6541.
74. Low, J. N.; Ferguson, G.; Wardell, J. L., Methyltriphenylstibonium tetrafluoroborate. *Acta Crystallogr., Sect. C: Cryst. Struct. Commun.* **2000,** *56,* e317.

75. Bordner, J.; Andrews, B. C.; Long, G. G., Fluoro(methyl)triphenylantimony, $C_{19}H_{18}FSb$. *Cryst. Struct. Commun.* **1976,** *5,* 801-804.
76. Wade, C. R.; Gabbaï, F. P., Fluoride Anion Chelation by a Bidentate Stibonium–Borane Lewis Acid. *Organometallics* **2011,** *30,* 4479-4481.
77. Hudnall, T. W.; Kim, Y.-M.; Bebbington, M. W. P.; Bourissou, D.; Gabbaï, F. P., Fluoride ion chelation by a bidentate phosphonium/borane Lewis acid. *J. Am. Chem. Soc.* **2008,** *130,* 10890-10891.
78. Wade, C. R.; Gabbaï, F. P., Cyanide and Azide Anion Complexation by a Bidentate Stibonium-Borane Lewis Acid. *Z. Naturforsch., B: J. Chem. Sci.* **2014,** *69,* 1199-1205.
79. (a) Brak, K.; Jacobsen, E. N., Asymmetric Ion-Pairing Catalysis. *Angew. Chem. Int. Ed.* **2013,** *52,* 534-561; (b) Zhang, Z.; Schreiner, P. R., (Thio)urea organocatalysis-What can be learnt from anion recognition? *Chem. Soc. Rev.* **2009,** *38,* 1187-1198.
80. Bulfield, D.; Huber, S. M., Halogen Bonding in Organic Synthesis and Organocatalysis. *Chem-Eur J* **2016,** *22,* 14434-14450.
81. Vogel, L.; Wonner, P.; Huber, S. M., Chalcogen bonding: an overview. *Angew. Chem. Int. Ed.* **2019,** *58,* 1880-1891.
82. (a) Chen, E. Y.-X.; Marks, T. J., Cocatalysts for metal-catalyzed olefin polymerization: activators, activation processes, and structure-activity relationships. *Chem. Rev.* **2000,** *100,* 1391-1434; (b) Piers, W. E., The chemistry of perfluoroaryl boranes. *Adv. Organomet. Chem.* **2004,** *52,* 1-76.
83. (a) Sen, S.; Gabbaï, F. P., An ambiphilic phosphine/H-bond donor ligand and its application to the gold mediated cyclization of propargylamides. *Chem. Commun.* **2017,** *53,* 13356-13358; (b) Franchino, A.; Martí, À.; Nejrotti, S.; Echavarren, A. M., Silver-Free Au(I) Catalysis Enabled by Bifunctional Urea- and Squaramide-Phosphine Ligands via H-Bonding. *Chem. Eur. J.* **2021,** *27,* 11989-11996; (c) Tzouras, N. V.; Gobbo, A.; Pozsoni, N. B.; Chalkidis, S. G.; Bhandary, S.; Van Hecke, K.; Vougioukalakis, G. C.; Nolan, S. P., Hydrogen bonding-enabled gold catalysis: ligand effects in gold-catalyzed cycloisomerizations in hexafluoroisopropanol (HFIP). *Chem. Commun.* **2022,** *58,* 8516-8519.
84. (a) Wolf, J.; Huber, F.; Erochok, N.; Heinen, F.; Guérin, V.; Legault, C. Y.; Kirsch, S. F.; Huber, S. M., Activation of a Metal-Halogen Bond by Halogen Bonding. *Angew. Chem. Int. Ed.* **2020,** *59,* 16496-16500; (b) Jónsson, H. F.; Sethio, D.; Wolf, J.; Huber, S. M.; Fiksdahl, A.; Erdelyi, M., Halogen Bond Activation in Gold Catalysis. *ACS Catalysis* **2022,** *12,* 7210-7220.
85. Zhou, B.; Gabbaï, F. P., Anion Chelation via Double Chalcogen Bonding: The Case of a Bis-telluronium Dication and Its Application in Electrophilic Catalysis via Metal–Chloride Bond Activation. *J. Am. Chem. Soc.* **2021,** *143,* 8625-8630.
86. Jones, J. S.; Gabbaï, F. P., Activation of an Au-Cl Bond by a Pendent Sb^{III} Lewis Acid: Impact on Structure and Catalytic Activity. *Chem. Eur. J.* **2017,** *23,* 1136-1144.
87. Christianson, A. M.; Gabbaï, F. P., A Lewis Acidic, π-Conjugated Stibaindole with a Colorimetric Response to Anion Binding at Sb(III). *Organometallics* **2017,** *36,* 3013-3015.
88. Christianson, A. M.; Rivard, E.; Gabbaï, F. P., $1\lambda^5$-Stibaindoles as Lewis acidic, p-conjugated, fluoride anion responsive platforms. *Organometallics* **2017,** *36,* 2670-2676.
89. Kubo, Y.; Kobayashi, A.; Ishida, T.; Misawa, Y.; James, T. D., Detection of anions using a fluorescent alizarin-phenylboronic acid ensemble. *Chem. Commun.* **2005**, 2846-2848.
90. Ke, I.-S.; Myahkostupov, M.; Castellano, F. N.; Gabbaï, F. P., Stibonium Ions for the Fluorescence Turn-On Sensing of F^- in Drinking Water at Parts per Million Concentrations. *J. Am. Chem. Soc.* **2012,** *134,* 15309-15311.
91. Usui, K.; Ando, M.; Yokogawa, D.; Irle, S., Understanding the On–Off Switching Mechanism in Cationic Tetravalent Group-V-Based Fluoride Molecular Sensors Using Orbital Analysis. *J. Phys. Chem. A* **2015,** *119,* 12693-12698.
92. Hirai, M.; Myahkostupov, M.; Castellano, F. N.; Gabbaï, F. P., 1-Pyrenyl- and 3-Perylenyl-antimony(V) Derivatives for the Fluorescence Turn-On Sensing of Fluoride Ions in Water at Sub-ppm Concentrations. *Organometallics* **2016,** *35,* 1854-1860.
93. Christianson, A. M.; Gabbaï, F. P., Anion sensing with a Lewis acidic BODIPY-antimony(V) derivative. *Chem. Commun.* **2017,** *53,* 2471-2474.
94. Kumar, A.; Yang, M.; Kim, M.; Gabbaï, F. P.; Lee, M. H., OFF–ON Fluorescence Sensing of Fluoride by Donor–Antimony(V) Lewis Acids. *Organometallics* **2017,** *36,* 4901-4907.
95. Kim, J.-B., Channelopathies. *Korean J. Pediatr.* **2014,** *57,* 1-18.
96. Ratjen, F.; Bell, S. C.; Rowe, S. M.; Goss, C. H.; Quittner, A. L.; Bush, A., Cystic fibrosis. *Nature Reviews Disease Primers* **2015,** *1,* 15010.
97. (a) Davis, A. P.; Sheppard, D. N.; Smith, B. D., Development of synthetic membrane transporters for anions. *Chem. Soc. Rev.* **2007,** *36,* 348-357; (b) Davis, J. T.; Okunola, O.; Quesada, R., Recent advances in the transmembrane transport of anions. *Chem. Soc. Rev.* **2010,** *39,* 3843-3862; (c) Gale, P. A.; Davis, J. T.; Quesada, R., Anion transport and supramolecular medicinal chemistry. *Chem. Soc. Rev.* **2017,** *46,* 2497-2519; (d) Wu, X.; Gilchrist, A. M.; Gale, P. A., Prospects and Challenges in Anion Recognition and Transport. *Chem* **2020,** *6,* 1296-1309; (e) Akhtar, N.; Biswas, O.; Manna, D., Biological applications of synthetic anion transporters. *Chem. Commun.* **2020,** *56,* 14137-14153.
98. Docker, A.; Langton, M. J., Transmembrane anion transport mediated by sigma-hole interactions. *Trends Chem.* **2023**, doi:10.1016/j.trechm.2023.06.001.
99. Lee, L. M.; Tsemperouli, M.; Poblador-Bahamonde, A. I.; Benz, S.; Sakai, N.; Sugihara, K.; Matile, S., Anion transport with pnictogen bonds in direct comparison with chalcogen and halogen bonds. *J. Am. Chem. Soc.* **2019,** *141,* 810-814.
100.Humeniuk, H. V.; Gini, A.; Hao, X.; Coelho, F.; Sakai, N.; Matile, S., Pnictogen-Bonding Catalysis and Transport Combined: Polyether Transporters Made In Situ. *JACS Au* **2021,** *1,* 1588-1593.
101.Park, G.; Brock, D. J.; Pellois, J.-P.; Gabbaï, F. P., Heavy Pnictogenium Cations as Transmembrane Anion Transporters in Vesicles and Erythrocytes. *Chem* **2019,** *5,* 2215-2227.
102.Smith, R. A. J.; Hartley, R. C.; Cocheme, H. M.; Murphy, M. P., Mitochondrial pharmacology. *Trends Pharmacol. Sci.* **2012,** *33,* 341-352.
103.Clarke, H. J.; Howe, E. N.; Wu, X.; Sommer, F.; Yano, M.; Light, M. E.; Kubik, S.; Gale, P. A., Transmembrane Fluoride Transport: Direct Measurement and Selectivity Studies. *J. Am. Chem. Soc.* **2016,** *138,* 16515-16522.
104.Park, G.; Gabbaï, F. P., Phosphonium Boranes for the Selective Transport of Fluoride Anions across Artificial Phospholipid Membranes. *Angew. Chem. Int. Ed.* **2020,** *59,* 5298-5302.
105.Cataldo, A.; Chvojka, M.; Park, G.; Sindelar, V.; Gabbai, F. P.; Butler, S. J.; Valkenier, H., Transmembrane transport of fluoride studied by time-resolved emission spectroscopy. *Chem. Commun.* **2023,** *59,* 4185-4188.
106.Agalakova, N. I.; Gusev, G. P., Fluoride-induced death of rat erythrocytes in vitro. *Toxicol. in Vitro* **2011,** *25,* 1609-1618.

TOC Graphic